

1 Improving regional ozone modeling through systematic evaluation
2 of errors using the aircraft observations during ICARTT

3
4 Marcelo Mena-Carrasco^{1*}, Youhua Tang^{1}, Gregory R. Carmichael^{1***}, Tianfeng**
5 Chai^{1**}, Narisara Thongbongchoo^{2*****}, J. Elliott Campbell^{1*****}, Larry Horowitz^{3*****},**
6 Jeffrey Vukovich^{4***}, William Brune^{5*****}, Jack E. Dibb^{6*****}, Glenn W.**
7 Sachse^{7***}, David Tan^{8*****}, Rick Shetter^{9*****}, Robert W.**
8 Talbot^{6***}, David G. Streets^{10*****}, Sarika Kulkarni^{1*****}**

9
10
11 1 Center for Global and Regional Environmental Research, University of Iowa, Iowa, USA

12 2 Department of Chemical Engineering Faculty of Engineering, King Mongkut's Institute

13 3 GFDL/NOAA

14 4 University of North Carolina at Chapel Hill.

15 5 Department of Earth Sciences, Pennsylvania State University

16 6 University of New Hampshire

17 7 NASA Langley Research Center

18 8 Georgia Institute of Technology

19 9 National Center for Atmospheric Research.

20 10 Argonne National Laboratory.

21 *401 IATL, Iowa City, IA 52242. E-mail: marcelo-mena@uiowa.edu , Telephone: 319-335-

22 3695, Fax: 319-335-3337 **402 IATL, Iowa City, IA 52242. E-mail: ytang@cgrer.uiowa.edu ,

23 Telephone: 319-335-3332, Fax: 319-335-3337. *401 IATL, Iowa City, IA 52242. E-mail:**

1 gcarmich@engineering.uiowa.edu , Telephone: 319-335-3332, Fax: 319-335-3337 ****427
 2 IATL, Iowa City, IA. E-mail: tchai@engineering.uiowa.edu , Telephone: 1-319-335-2063 , Fax:
 3 1-319-335-3337.***** Chalongkrung Rd., Ladkrabang, Bangkok 10520, Thailand. E-mail:
 4 ktnarisa@kmitl.ac.th , Telephone: +66-2739-2417, Fax: +66-2-739-2417 ext 4. *****401
 5 IATL, Iowa City, IA 52242. E-mail: cae@engineering.uiowa.edu , Telephone: 319-335-3695,
 6 Fax: 319-335-3337 *****Princeton University Forrestal Campus, 201 Forrestal Road,
 7 Princeton, NJ 08540-5063. E-mail: larry.horowitz@noaa.gov , Telephone: 1-609-452-6520 ,
 8 Fax: 1-609-987-5063. *****670 Bank of America, Carolina Environmental Program,
 9 University of North Carolina at Chapel Hill, Chapel Hill, NC 27599-6116. E-mail:
 10 jeff_vukovich@unc.edu, *****Department of Meteorology, 504 Walker Building,
 11 University Park, PA 16802. E-mail: brune@meteo.psu.edu , Telephone: 1-814-865-3286,
 12 ***** 56 College Road, James Hall, Room 121, Durham, NH 03824-3589. E-mail:
 13 jack.dibb@unh.edu , Telephone: 1-603-862-1718, Fax: 1-603-862-2649. *****NASA
 14 Langley Research Center, Hampton, VA 23681-0001. E-mail: Glen.W.Sachse@nasa.gov
 15 *****ES&T, Room 3242, School of Earth and Atmospheric Sciences, Atlanta, GA,
 16 30332-0340. E-mail: dtan@eas.gatech.edu , Telephone: 1-404-385-1821, Fax: 1-404-894-5638.
 17 *****1850 Table Mesa Dr, Boulder, CO 80305. E-mail: shetter@ucar.edu , Telephone:
 18 1-303-497-1480, Fax: 1-303-497-1411. ***** 9700 South Cass Avenue, Argonne, IL
 19 60439. Email: dstreets@anl.gov *424 IATL, Iowa City, IA 52242. E-mail: [kulkarni@uiowa.edu](mailto:sarika-

 20 <a href=)
 21
 22
 23

1 Abstract:

2 During the operational phase of the ICARTT field experiment in 2004, the regional air
3 quality model STEM showed a strong positive surface bias, and a negative upper troposphere
4 bias (compared to observed DC-8 and WP-3 observations) with respect to ozone. After updating
5 emissions from NEI 1999 to NEI 2001 (with a 2004 large point sources inventory update), and
6 modifying boundary conditions, surface model bias decreased from 11.21 to 1.45 ppbv for the
7 NASA DC-8 observations and from 8.26 to -0.34 for the NOAA WP-3. Improvements in
8 boundary conditions decreased the upper troposphere negative ozone bias, while improving
9 model performance for CO by accounting for biomass burning emissions. Lightning NO_x
10 emissions improved upper troposphere modeling of nitrogen species. Ozone bias was shown to
11 be highly correlated to NO_z, NO_y, and HNO₃ bias. Interpolation of bias information through
12 Kriging showed that decreasing emissions in SE United States would decrease regional ozone
13 bias and improved model correlation coefficients. Observed and modeled ozone production
14 efficiencies for the DC-8 were very similar (7.8) showing that model chemistry was appropriate,
15 and that recurring ozone bias is due to overestimated NO_x emissions. WP-3 observed and
16 measured ozone production efficiencies differed (3.49 and 5.28), respectively.

17

18 **KEY WORDS:** ozone air pollution modeling kriging ICARTT INTEX-A NEAQS bias STEM

19 **INDEX TERMS:** 0345 Pollution—urban and regional; 0365 Troposphere—composition and
20 chemistry; 3337 Numerical modeling and data assimilation

1 **1. Introduction:**

2 Air pollution models have been used to predict air quality during numerous field
3 campaigns [Bates *et al.*, 1998; Jacob *et al.*, 2002; Ramana *et al.*, 2004], with the objective to
4 both place air pollution in a geographical context and, as the data is collected, evaluate our
5 current understanding of atmospheric processes [Kiley *et al.*, 2003] and anthropogenic and
6 biogenic emissions [Carmichael *et al.*, 2003]. During the summer of 2004, the ICARTT
7 (International Consortium for Atmospheric Research on Transport and Transformation) field
8 experiment was performed (<http://www.al.noaa.gov/ICARTT>), which included a NASA
9 experiment called INTEX-A (Intercontinental Chemical Transport Experiment-A), and a NOAA
10 experiment called NEAQS/ITCT-2k4 (New England Air Quality Study - Intercontinental
11 Transport and Chemical Transformation, 2004). During this period NASA DC-8 and NOAA
12 WP-3 aircraft each performed 18 research flights over the continental US, with a special focus on
13 the Northeastern United States. Figure 1 shows the flight tracks of the DC-8 during the mission,
14 and the altitude at which the aircraft flew. Figure 2 shows the flight tracks of the WP-3 aircraft,
15 which flew at lower altitudes, mostly over the NE United states. More details about the aircraft
16 measurements and main finding are available in this issue [Singh *et al.*, 2006]. During the field
17 experiment operations the University of Iowa STEM model [Carmichael and Peters, 1991; Tang
18 *et al.*, 2004] was run. The forecasts showed a persistent positive bias (modeled-observed) for
19 ozone [Mc Keen *et al.*, 2005] in comparison to surface sites in the AIRMAP network
20 (<http://airmap.unh.edu/>), and in comparison to the aircraft platform observations. The objective
21 of this paper is to show model performance in relation to ozone and its precursors was improved
22 through systematic analysis of model prediction with the observed data to evaluate where model
23 error persists, and how ozone model error is related to model error of other species. The paper

1 also demonstrates how geospatial interpolation through Kriging can be used along with other
2 statistical analysis to enhance model performance.

3 **2. Methodology**

4 In this study we used the STEM-2K3 model. The model features the lumped species
5 SAPRC99 chemical mechanism [*Carter, 2000*] with an on-line photolysis solver, and the
6 SCAPE II aerosol solver. Meteorological inputs to the model came from MM5 using the AVN
7 data during forecasting and NCEP FNL (Final Global Data Assimilation System) analyzed data
8 during post-analysis. For this study the model domain was the continental United States, using a
9 60km resolution, 62 cells in longitude, and 97 cells in latitude. The model had 21 vertical layers,
10 extending from the surface to 100hPa using 0.999, 0.9965, 0.9925, 0.985, 0.97, 0.945, 0.91, 0.87,
11 0.825, 0.77, 0.71, 0.65, 0.59, 0.53, 0.47, 0.41, 0.35, 0.285, 0.21, 0.125, and 0.04 in sigma
12 coordinate. The Grell cumulus parameterization [*Grell et al., 1995*] and the MRF planetary
13 boundary layer parameterization [*Hong et al., 1996*] were used for the MM5 runs.

14 During the operational portion of the experiment, anthropogenic emissions were taken
15 from the U.S EPA National Emissions Inventory for the base year of 1999 (NEI 1999) [*EPA,*
16 2006] while the 2001 update of the same (NEI 2001) was used for the post analysis stage. It
17 should be noted that NEI 2001 has lower emissions in CO, NO_x, and SO₂ than NEI 1999 (Table
18 1). Modifications were still needed since the simulations with NEI 2001 systematically
19 underestimated light alkanes, and overpredicted aromatic species. The large point source
20 emissions (LPS) used were the updated inventory by Gregory Frost at NOAA Earth Systems
21 Research Laboratory (personal communication), which represents emissions for 2004, the year
22 of the campaign. Upper troposphere lightning NO_x emissions were added to the model in post-
23 analysis based on the National Lightning Detection Network (NLDN), relating emissions to

1 signal strength and multiplicity of flashes. Further information about lightning emissions can be
2 found in this issue [*Tang et al.*, 2006]. Biogenic emissions were estimated using BEIS 2
3 (Biogenic Emissions Inventory System) which generates time-variable isoprene and
4 monoterpene emissions driven by meteorological variables from MM5. Forest fires that occurred
5 during the ICARTT period were largely outside our regional model domain (in Alaska and
6 Northwestern Canada), therefore their influence was incorporated through lateral boundary
7 conditions from MOZART GFDL (NOAA GFDL) [*Horowitz et al.*, 2003] during the forecast
8 (which used climatological fire emissions), and from MOZARTT NCAR [*Pfister et al.*, 2005] in
9 the post analysis, which used assimilated CO values from MOPITT (Measurements of Pollution
10 in the Troposphere instrument on board the TERRA satellite) to constrain the fire emissions.

11 The post analysis work was focused on improving model performance by carefully
12 comparing predictions with observations, and to use the error information to identify aspects of
13 the model in need of improvement. Model sensitivity studies were done for factors with
14 significant uncertainty including boundary conditions, anthropogenic emissions inventories, sea
15 salt emissions, lightning NO_x emissions, and dry deposition rates. From these various runs three
16 were selected for detailed analysis in this paper. These are the 1) operational forecasting
17 conditions (Forecast, NEI 1999), 2) the most updated emissions inventory (NEI2001-Frost LPS),
18 and 3) a modification of that emissions inventory (NEI2001-Frost LPS-Modified). Table 2
19 shows a summary of the model parameters for the different scenarios compared in this study.
20 Table 1 shows the total column anthropogenic CO emissions for the domain decreased by 40%
21 from NEI 1999 to NEI 2001, and that Frost LPS increases CO with respect to NEI 2001. The
22 surface NO_x emissions decreased significantly from NEI 1999 to NEI 2001 (~30%). Figure 3
23 shows the domain column emissions of NO_x for NEI 1999 (Left panel), NEI2001-Frost LPS

1 (Center Panel, and the decrease of emission from NEI 1999 to NEI 2001-Frost LPS (Right
2 panel).

3 The results from runs with these different conditions for the period July 1 to August 18,
4 2004, which includes a model spin up period and which covers the span of the DC-8 and WP-3
5 flights 3-20 for ICARTT, are discussed in this paper. Merged data for both measurement
6 platforms were re-sampled from a 1 second to a 3 minute resolution, and compared to
7 interpolated data from the 3 h, 60km, and 21 variable vertical resolution model output.

8 **2.1 Kriging**

9 Kriging has been previously used for interpolating surface measurements of ozone, and
10 particulate matter for health studies, and estimation of exposure [*Liao et al.*, 2006] and to
11 generate maps of air pollution based on discrete measurements, such as the AIRNOW network
12 [*EPA*, 1999]. Kriging produces a surface of predicted values and uncertainty using a semi-
13 variogram (in this case exponential), which relates percent bias (bias/mean observed*100) metric
14 and distance of the target point to nearby points. We used ArcGIS 9.0 to carry out ordinary
15 Kriging with the 50 nearest points, without restricting distance between points. Analysis to
16 altitudes less than 4000m. This assumes that the vertical variability in this range is smaller than
17 the horizontal variability. The continuous surface output of Kriging provides geospatial context
18 to bias, and allows the comparison of related bias of different species to ozone.

19 **3. Model Performance**

20 The surface ozone forecasted during ICARTT has been compared with surface
21 observations and showed a significant high bias for daytime values (~15 ppbv) [*McKeen et al.*,
22 2005]. As discussed above, during the forecast period we used the NEI 1999 emissions and
23 boundary conditions from the MOZART GFDL global atmospheric chemistry forecast. We

1 anticipated that errors would occur due to the fact that the experiment was conducted in 2004,
2 and that the actual emissions would differ from the 1999 values used in the forecast. Furthermore
3 in the summer of 2004 significant fires occurred in Alaska and Canada. The fire emissions used
4 in the forecasts relied on climatological fires and thus underestimated the actual emissions from
5 fires for 2004. Additionally, it was found in post analysis that the dry deposition velocities for
6 agricultural crops were set to low growing season conditions. These factors all contributed to
7 forecast errors.

8 Below we compare the forecasted values with aircraft observations. We also compare the
9 results from model runs where the dry deposition velocity has been corrected, and where the
10 emissions and boundary conditions have been updated.

11 **3.1 Statistical Performance for all flights**

12 The predictions of O₃, CO and NO_y for the various simulations cases are compared with
13 the DC8 observations in Figure 4 and Table 3. For these comparisons all data from Flights 3-20
14 are combined together and analyzed by altitude. The predicted values are interpolated to the
15 same spatial location of the observations using tri-linear interpolation. In general the forecast
16 values show a significant positive bias in predicted ozone at altitudes below ~4 km, and a high
17 negative bias above this altitude. The mean bias below 1 km is ~ 11 ppbv, similar, but slightly
18 lower to the values found from the analysis of the surface AirNow observations. Comparable
19 patterns are found in the forecast for CO and NO_y, with high values at low altitudes and low
20 values at high altitudes. The post analysis runs show significant improvements in the predictions
21 at altitudes below 4 km. In the case of ozone the NEI01-Frost LPS case shows that the low
22 altitude bias is reduced to less than 3 ppbv. The bias in the mid troposphere (4-8 km) is also
23 reduced (by ~ 50%). Similar improvements are found for CO. Improvements in the bias above

1 4km are largely due to the updated global boundary conditions (MOZART-NCAR), which
2 include a better representation of the biomass burning emissions from Alaska and northern
3 Canada. Tang et al. (2006) evaluated the impact of boundary conditions on model performance
4 using results from three different global models and found that they dominate the performance of
5 the regional model at these altitudes. The remaining bias reflects the performance skills of the
6 global models used. For NO_y , the bias in the near surface regions is reduced, but by a much
7 smaller rate while the bias at higher altitudes decreases significantly. The improvements at the
8 higher altitudes reflect the importance of including lightning NO_x emissions. The comparison of
9 the ratio of the standard deviation to the mean value of the predictions and those for the
10 observations shows that the model exhibits a variability that is similar to that of the observations.

11 Similar results are found for the WP-3 comparisons (Table 4). As shown by comparing
12 Figures 1 and 2, the flight operations of the WP-3 and DC8 were different, with the WP-3
13 focused largely on the northeast US. This along with the flight altitude differences lead to
14 differences in the statistics in the observed distributions of the DC8 and WP-3 data. For example,
15 the WP-3 low altitude values on average are higher. In the case of ozone and CO the mean
16 observed values from all flights were 56 and 158 ppbv for the WP-3 and 49 and 138 ppbv,
17 respectively, for the DC8. The mean bias in the forecast for ozone for the WP-3 was 8.3 ppbv,
18 compared to 11 ppbv for the DC8 comparison. Correlation coefficients for both aircraft were
19 very similar for the 0-1km range (0.71 for DC-8, and 0.69 for WP-3). For the post analysis
20 simulation NEI2001-Frost LPS the bias in predicted ozone at low altitudes was reduced to 0.28
21 ppbv and the correlation was increased to 0.66. The mean bias values for the lower altitude
22 predicted for this case for CO and NO_y were also reduced significantly (by ~90 and 70%,
23 respectively). For the 1-4km range the ozone correlation improved (R increases from 0.57 to

1 0.65) and the mean bias decreased from 4.9 to -0.6. CO predictions also improved with R
2 increasing from 0.52 to 0.66, and bias decreasing from 28.37 to 8.79. Note that the CO bias
3 remains significant for the WP-3 flights, from which we can infer that there is still a systematic
4 over prediction of CO for the area that was sampled by WP-3, largely in the NE United States.
5 For the 4-8km range we can see that emissions and boundary condition improvements
6 significantly enhanced ozone modeling performance, with R increasing from 0.15 to 0.46, and
7 bias decreasing from -16.2 to -7.8. Similarly CO performance increased due to boundary
8 conditions incorporating biomass burning (R increases from 0.11 to 0.36). Lightning NO_x
9 emissions in the upper troposphere improved the modeling of reactive nitrogen species,
10 decreasing the negative bias in the upper troposphere.

11 It is important to note that while the predicted biases in NO_y were reduced significantly in
12 the post-analysis runs, they remain quite high (~1ppbv overprediction when averaged over all
13 altitudes for the DC8 and WP-3 observations). The NO_y distributions and their comparison with
14 various models used during ICARTT are discussed in detail in Singh et al. (this issue). In Figure
15 5 we plot the observed and predicted contribution of individual species to NO_y for the DC8
16 observations and for the NEI2001-Frost LPS simulations. This plot shows that the predicted
17 contributions are similar to those observed. Nitric acid is shown to compose the largest NO_y
18 fraction below ~4km, above which PAN contributes from 40 to 50% up to about 8 km. In the
19 upper troposphere NO contributes to a significant fraction of nitrogen. Within the boundary layer
20 PAN and NO₂ contribute ~20% to NO_y. The relative contribution of NO in comparison to NO₂
21 increases with altitude. The predicted distributions differ in comparison with the observations in
22 that the absolute contributions of HNO₃ are lower than those observed. In addition the predicted

1 contribution of NO increases with altitude at a slower rate than that observed. This fact is
2 probably related to the treatment of the lightning NO_x emissions.

3 The fact that the predicted distributions compare favorably with the observations, suggest
4 that the NO_x emissions in the model are still higher than the actual emission in the summer of
5 2004. While the emissions used in this simulation have the large point source sector updated to
6 2004, emissions from the other sectors are based on 2001 values. The transportation sector is the
7 major emitting sector for NO_x and is trending downward. So it is most likely that NO_x emissions
8 in 2004 are actually lower than those in 2001. To reflect this case we performed an additional
9 simulation (NEI2001–Frost LPS-Modified case) where the NO_x emissions were reduced by an
10 additional 12% with respect to total NO_x (but by 40% for area NO_x emissions for selected states,
11 as is shown in Table 1). The results of this case are also presented in Tables 3 and 4, and Figure
12 4. The effect of this reduction in NO_x emissions is to further reduce by ~20% the bias in NO_y.
13 Since ozone production in the ICARTT region is largely NO_x limited, this reduction in NO_x
14 emissions also reduced the mean ozone levels by ~ 1ppbv, and further reduced the bias in the
15 lowest layers by 50% (to 1.45 ppbv for the case of the DC8), compared to the NEI2001-Frost
16 LPS case.

17 The modeling of volatile organic compounds (VOC) has always been a challenge due to
18 the uncertainty of VOC emissions inventories in the US [Parrish *et al.*, 2006]. In the simulations
19 aromatic species are represented through the SAPRC99 lumped species [Carter, 2000] as ARO1
20 (Aromatics with $k_{OH} < 2 \text{ ppm}^{-1} \text{ min}^{-1}$), and ARO2 (Aromatics with a $k_{OH} < 2 \text{ ppm}^{-1} \text{ min}^{-1}$). ARO1
21 represents benzene and toluene, while ARO2 represents 8 to 9 carbon aromatics. Predictions of
22 ARO1 and ARO2 were compared to the sum of benzene and toluene and the sum of all 8 carbon
23 aromatics, respectively. During the forecast stage, the model showed a small overprediction of

1 ARO1 near the surface which, after updating the emissions inventories, switched to an
2 underprediction (Figure 6). At altitudes over 2km, all model scenarios showed a negative bias for
3 the prediction for ARO1, ethene, ethane, and propane, largely due to errors in the global model
4 boundary conditions with contributions from errors from imprecise treatment of convective
5 events. Note that ARO1 species were only sparsely measured in the upper troposphere (6 points
6 in the 4-8km range, and 3 points in the 8-12km range in our model domain), so conclusions for
7 those ranges are highly uncertain.

8 Figure 7 shows a quantile-quantile plot of observed and modeled O_3 for the DC-8 and P-3
9 (only the 0-80ppbv range was considered due to limited data above that range). The forecast
10 values show a systematic overprediction across the whole range, while the NEI2001-Frost LPS-
11 Modified case shows a lower overprediction in the range of 20-40ppbv, and very good
12 agreement for values over 50ppbv, which represented the vast majority of the points sampled
13 (more than 80% of the observations in WP-3 exceeded 50ppbv). This slight improvement in
14 modeling the low values reflect the influence of boundary conditions and the relatively coarser
15 resolution used in these comparisons.

16 The overall performance of the NEI2001-Frost-LPS prediction with respect to 35
17 different observed parameters for the DC-8 data are show in Figure 8. Plotted are the correlation
18 coefficients, R , for the 0-1km and 1-4km altitude range. Temperature and wind speed have the
19 largest values for both altitude ranges. In the 0-1km range sulfate, HCHO, O_3 , PAN and RH have
20 R values of 0.6. The nitrogen oxide species have R values greater than 0.4 while most of the
21 primary hydrocarbons have R values less than 0.35. In general the R values, reflecting model
22 performance, decreases with altitude.

1 **4. Case studies**

2 The results above provide a mission wide perspective. NEI2001-Frost LPS-Modified
3 ozone bias is shown on a flight by flight basis in Figure 9. Generally the bias in the lowest layers
4 is lower than 5ppbv, while the bias in the 8-12 km range is large, and particularly high in flights
5 3, 11, 15, 16, and 17. This is a reflection of the boundary conditions from the global model. Tang
6 et al. (this issue) shows that boundary conditions varied greatly among global models, and
7 depending on the global models used the ozone bias in the upper troposphere varied from a large
8 negative to large positive values. Details for specific flights were also analyzed. Figure 10 shows
9 how model performance improved during DC-8 flights 12 and 14 (July 25 and 31, 2004), in
10 which the low altitude positive bias decreases significantly (due to emissions improvement),
11 along with a decrease in the upper altitude negative bias, due to improved boundary conditions.
12 Figure 11 shows how model performance improves for WP-3 flight 11, in which the positive low
13 altitude bias (less than 4km) decreases from 15 ppbv to 1 ppbv, and negative bias
14 (altitude>4000m) improves from -16.6 to 6.6, while increasing the R correlation coefficient for
15 the flight from -0.02 to 0.67.

16 **5. Analysis of model error**

17 The relationship between model errors is a key step in understanding model behavior and
18 identifying model deficiencies. This information is also becoming increasingly important as
19 estimates of error covariance are an important aspect of chemical data assimilation [*Chai et al.*,
20 2006]. The ICARTT experiment produced observations for a large spectrum of species that are
21 involved in the photochemical oxidant cycle. Thus it is possible to use these data to explore the
22 relationships between the calculated ozone errors with errors in other species. In this section we
23 analyze the correlations between model errors (modeled-observed) for ozone and other species.

1 **5.1. Correlation between model biases.**

2 The correlations between the ozone bias and the bias in a variety of species were
3 calculated using the DC8 data and the results are presented in Table 5. Shown are results for the
4 post analysis simulation NEI2001-Frost LPS.

5 For altitudes < 1km PAN, CO, MEK, and HNO₃ show the highest correlation (0.60, 0.51,
6 0.48, and 0.47, respectively). In the altitude range of 1-4km the influence of MEK and CO
7 decreases significantly, and biases of PAN, NO_z, NO_y, and HNO₃ show the highest correlation
8 coefficients to ozone bias (0.64, 0.57, 0.55, and 0.45, respectively). In the 4-8km range the bias
9 correlation coefficients generally decrease, with nitrogen species NO_z, NO_y, PAN, and NO₂
10 presenting the highest values.

11 The correlation of model errors has many similar aspects as the correlations between
12 observed ozone levels and the various species. Table 5 also shows that the observed ozone
13 concentrations at low altitude (0-1km) are most strongly correlated to HNO₃ (R=0.86), Ethyne
14 (R=0.75), NO_z (R=0.77), CO (R=0.70), acetone (R=0.68), and MEK (R=0.65). These species
15 represent the general importance of ozone precursors and indicators of the photochemical
16 oxidant cycle. The correlations are very small for short lived species such as NO, propene and
17 isoprene (-0.03, -0.06 and -0.03, respectively). These relationships change for the 4-8km range,
18 where only nitrogenous species concentrations show the highest correlation to ozone, with NO₂
19 (R=0.48), NO_y (R=0.48), NO_z (R=0.47), and PAN (R=0.39). At higher altitudes (8-12km)
20 correlations HNO₃ (R=0.67), NO_z (R=0.42), NO_y (R=0.27) and with RH (-0.35) and wind speed
21 (R=0.14) are the highest.

22 A factor analysis (factor criteria of 90% variance) using the observed values for the DC-8
23 at altitudes below 1km was performed to identify the underlying relationships between ozone

1 and other species. The factor with the largest score is shown in Figure 12. This factor contains a
2 spectrum of species related to ozone and its precursors and clustered to clusters together those
3 photochemical factors identified in Table 5. The same analysis was conducted using the
4 predicted values (NEI2001-Frost LPS-modified) to relate species to ozone. In general the factors
5 identified by the model predictions show many similarities to those based on observations
6 suggesting that the modeled processes are capturing many of the ozone relationships in the real
7 atmosphere. A factor analysis was performed for the model errors (bottom of Figure 12). The
8 clustering of errors shows a structure similar to that for the species dependencies.

9 **6. Bias in a regional context**

10 Geographical context is given to the point bias estimations (observation-modeled) by
11 interpolating them through Kriging, generating a continuous surface. Data was restricted to the
12 0-4km range, for all DC-8flights. The previous section suggested which variables need to be
13 improved to lower ozone bias. The interpolated bias surface gives guidance towards where
14 emissions inventories should be modified. The surface of ozone bias is shown in Figure 13. For
15 the forecast (left panel) we observe that during the forecast there was a positive bias in the
16 Western and Eastern United States with bias in the range of 15-20%. The biases in CO, NO₂,
17 HNO₃, and PAN, which showed strong correlation with ozone bias as discussed previously, was
18 also analyzed. Wherever ozone presented a positive bias in the forecast (Figure 13, left panel)
19 CO, NO₂, HNO₃, and PAN (Figures 14 to 17, left panel) also presented positive biases, this
20 particularly clear for NO₂ (Figure 15) where the bias in some regions of Ohio, North Carolina
21 and Virginia are as large as 400-500%. When the emission inventories were modified, updating
22 to NEI 2001 and the large point sources (Frost LPS), the ozone bias decreased to ~ 5-10% across
23 domain (Figure 13, center panel), with large decreases in the regions of high positive bias. The

1 bias in CO was reduced through the continental U.S., along with the bias of NO_y species.
2 However positive bias persisted for ozone and NO_y components. To further reduce the bias, an
3 additional simulation was conducted with a 60% decrease of NO_x area emissions (12%
4 reduction of total NO_x emissions) for Alabama, Mississippi, Georgia, North Carolina, South
5 Carolina, Tennessee, West Virginia, Indiana, and Ohio, since these states presented the highest
6 bias in NO₂, NO_y, and NO_z according to the Kriging results. The results of this run showed
7 enhancement of correlation factors for nitrogen species, particularly for HNO₃, and NO_y, while
8 decreasing their positive bias. As shown in Figure 13, right panel, the ozone bias decreased to a
9 range of -10 to 10% for most of the continent, with large portions showing bias in the -2 to 2%
10 range. The offshore ozone positive bias persists, but to lesser geographical extent, and lower
11 magnitude than the NEI 2001 scenario, and the forecast scenario. NO₂ for this same scenario
12 decreases its regional bias to less than 50% over large portions of the domain (Figure 14). Figure
13 16 shows that HNO₃ bias also decreases significantly with the updated and modified emissions,
14 with some areas presenting a negative bias. Figure 17 shows that PAN bias decreased in South
15 Carolina, North Carolina, and Virginia from 300-400% to 100-200%, in accordance to locations
16 where the ozone bias was decreased.

17 Special notice must be taken Figure 13, which shows that forecast CO, using NEI1999
18 presented positive biases of 30-40% for the Western portion of the United States, which
19 decreased to 10-20% using the NEI 2001. Negative CO bias over Minnesota decreased from -30
20 to -20% to -20 to -10%. The offshore Atlantic positive CO bias decreased from 20-40% to the
21 10-30% range and from 10-20% to -5 to 5% for the Southeastern US.

1 **7. Ozone production efficiency**

2 Up to now we have shown that the ozone bias was strongly correlated to NO_z and NO_y
3 bias. We have also discussed that there is geographical concordance of ozone bias with NO_z bias.
4 Previous work has related these variables [*Kleinman, 2005; Trainer et al., 1993*], in a
5 relationship for ozone production efficiency (OPE), which for the purposes of this analysis is the
6 ratio of odd oxygen ($\text{NO}_2 + \text{O}_3$) to NO_z . In Figure 18 the ozone production efficiency for the
7 observed and predicted values for data points less than 4000 m is plotted. For the DC-8 data the
8 observed OPE is 7.8, while the forecast, NEI2001-Frost LPS, and NEI2001-Frost LPS-Modified
9 cases have OPE's of 6.7, and 7.8, respectively. The observed ozone production efficiency for the
10 DC-8 data is similar to those observed for Houston (OPE=7.4) [*Kleinman et al., 2002*]. The
11 ozone production efficiency in the area sampled by WP-3 is lower than the DC-8 (Observed
12 OPE=3.49, Modeled OPE=5.28), which reflects fact that the area sampled was closer to emission
13 source regions in the North East.

14 **8. Sensitivity studies**

15 The fact that the modeled and observed production efficiencies are similar suggests that
16 the underlying ozone relationships of the model are sufficiently accurate to support sensitivity
17 studies. Further insights into ozone production can be seen by comparing the change in ozone to
18 changes in emissions. The mean predicted near surface ozone (0-1km) values for the NEI 2001
19 Frost LPS-Modified is shown in Figure 19. The sensitivity of O_3 to increases in emissions of
20 precursors is shown also shown in Figure 19. These simulations were done for the period of July
21 21 to August 18, 2004, in the absence of VOC, CO, and reduced NO_x . Ozone is most sensitive to
22 changes in NO_x , especially in the Midwest, where ozone per Tg of NO_x increases by 10-20ppbv
23 (Note that NO_x sensitivity was calculated based on 30% reduction of total NO_x). In the Northeast

1 US ozone is equally sensitive to NO_x and anthropogenic VOC, while in large parts of the western
2 US, ozone is more sensitive to VOC. CO effects are similar to VOC, but smaller on a per Tg
3 basis. Since CO emissions are larger than VOC, in total CO effects on ozone can be in the same
4 order of magnitude. Figure 20 shows that VOC and CO contribute to a large portion of ozone
5 formation in portions of the Northeast United States.

6 As pointed out above, NO_x plays an important role in ozone production. Furthermore an
7 appreciable fraction of NO_y is composed of PAN (representing ~ 20% near the surface and ~50%
8 at 6-8 km altitudes, Figure 5), and ozone levels and errors were shown to be significantly
9 correlated with those for PAN. PAN plays important roles as both a key photochemical product
10 and as a reservoir for NO_x . To assess the role of PAN on ozone production we conducted a
11 simulation where PAN levels within the regional domain (but not in the boundary conditions)
12 were continuously set to zero. In this way the formation of PAN was allowed, but the thermal
13 decomposition source of NO_x was blocked. The impact of PAN on predicted mean surface
14 ozone for the month of July is shown in Figure 21. This indirect ozone production pathway of
15 PAN via production of NO_x is estimated be over 20% throughout the continental US with large
16 regions with values between 30-50%. This impact extends to all altitudes with values exceeding
17 8% throughout the domain at an altitude of 5.6 km. Differences become small above this height
18 as the PAN levels are dominated by the boundary conditions values, which were not changed.
19 The results point out the importance of accurately prediction PAN levels, which requires the
20 close coupling between the regional and global models, as PAN sources and sinks reflect process
21 occurring throughout the vertical extent of the atmosphere and over large geographic scales.

22

1 Additional simulations were performed to investigate the sensitivity of the model to other
2 important parameters. Simulations were performed for the Eastern US using a 12km horizontal
3 resolution. The biggest impact was found near the surface for the 12km resolution. For the 0-
4 1km range the mean for the WP-3 increased by 3ppb with a slight increase in correlation to
5 (R=0.65). For CO the 12 km resolution increased the mean value by 5ppb and also increased the
6 correlation coefficient. Biogenic emissions represent an additional source of uncertainty. We
7 repeated a simulation using the BIES3 biogenic emissions algorithm, which led to higher
8 biogenic emissions. Under these conditions the near surface ozone increased by 3ppbv along the
9 East Coast, and 1 ppbv throughout the Eastern US. Isoprene values increased by 1 ppbv and CO
10 by 10 ppbv. The impact of dry deposition velocities was also studied and found to be large. Near
11 surface ozone values in the agricultural regions in the Midwest and plains states changed by 10-
12 20ppb when dry deposition velocities for agricultural land were varied from low growing to high
13 growing season.

14 **9. Conclusion**

15 ICARTT aircraft observations were used to evaluate and improve ozone prediction for
16 the STEM model. Model performance was enhanced by updating emissions inventories from
17 NEI 1999 to NEI 2001, and updating large point source emissions for 2004. This results in a
18 decrease in low altitude (0-1km) mean ozone bias from 11.21 to 1.45 ppbv in comparison to DC-
19 8 observations and from 8.26 to -0.34 ppbv for the WP-3 data. The upper troposphere ozone
20 negative bias persisted, which is related to boundary conditions, but the magnitude of the bias
21 has decreased.

22 Improvements in boundary conditions from global models, which accounted for biomass
23 burning emissions, improved model performance for CO in the upper troposphere, in comparison

1 to the forecast stage. Improvement in lightning NO_x emissions in the upper troposphere
2 increased the correlation coefficients for the 4-12km altitude range for the DC-8 and WP-3.

3 Nitrogen species, namely NO_y , NO_z , HNO_3 , presented positive bias during forecast stage,
4 which decreased during post-analysis. Reductions in these biases resulted in reduction of ozone
5 bias, especially in the 0-4km range. However a persistent high NO_y bias suggests that the NEI
6 2001 NO_x emissions are to

7 The use of ozone bias correlation to the bias of other species gives information on what
8 species affect ozone bias the most. The use of interpolated bias data through Kriging was shown
9 provide a geospatial analysis of these biases. Taking both into account the information can help
10 guide regional modification of emissions.

11 Predicted ozone production efficiency (OPE) was similar observed OPE, with the latest
12 model run showing an OPE of 7.83 in comparison to observed OPE of 7.79 for the DC8. Both
13 the observed OPE for the WP-3 was lower than the DC-8 (3.49) and the modeled OPE (5.28)
14 suggesting that the area sampled by the WP-3 was closer to the source regions of NO_x .

15 The sensitivity of the ozone predictions to dry deposition velocity, biogenic emissions,
16 and grid resolution were also shown to be significant.

17 Further improvements in the prediction of ozone require efforts to further improve the
18 emissions estimates.

19 **Acknowledgements:**

20 This work was supported by NASA GTE INTEX-A and NOAA NEAQS-ITCT-2k4.

1 **References:**

- 2
- 3 Bates, T. S., B. J. Huebert, J. L. Gras, F. B. Griffiths, P. A. Durkee, International Global
4 Atmospheric Chemistry (IGAC) Project's First Aerosol Characterization Experiment
5 (ACE 1): Overview, *J. Geophys. Res.*, 103(D13), 16297-16318, 10.1029/97JD03741,
6 1998.,
- 7 Carmichael G. R., et al., Evaluating regional emission estimates using the TRACE‐P
8 observations, *J. Geophys. Res.*, 108 (D21), 8810, doi:10.1029/2002JD003116, 2003.
- 9 Carmichael, G. R., Y. Tang ,G. Kurata,I. Uno, D.G. Streets, N. Thongboonchoo, J. Woo, S.
10 Guttikunda, A. White, T. Wang, D.R. Blake, E. Atlas, A. Fried, B. Potter, M.A. Avery,
11 G.W. Sachse , S.T. Sandholm, Y. Kondo, R.W. Talbot, A. Bandy, D. Thornton, A.D.
12 Clarke Evaluating regional emission estimates using the TRACE-P observations, *Journal*
13 *Of Geophysical Research-Atmospheres*, 108, 8810, 2003.
- 14 Carter, W. P. L. (2000), Documentation of the SAPRC-99 Chemical Mechanism for VOC
15 reactivity assessment, Final Report to California Air Resources Board Contract No. 92-
16 329, University of California, Riverside, May 8, 2000.
- 17 Chai, T., G.R. Carmichael, Y. Tang, A. Sandu, D.G. Streets, Evaluating and improving regional
18 emission estimates using the ICARTT observations, *Journal Of Geophysical Research-*
19 *Atmospheres*, This Issue.
- 20 EPA, Report of the December 15, 1999 EPA Satellite Forum on Ozone Monitoring, Mapping,
21 and Public Outreach, <http://epa.gov/empact/techtransfer/satellite.htm>, 1995 (Accessed
22 June 2006).
- 23 EPA (2006), 1999 National Emission Inventory,
24 <http://www.epa.gov/ttn/chief/net/1999inventory.html#final3crit> (Accessed June 2006).
- 25 Grell, G., J. Dubhia, D.R. Stauffer, Description of the Fifth Generation Penn State/NCAR
26 Mesoscale Model (MM5), <http://cng.ateneo.net/cng/wyu/resources/mm5/desc/cover.pdf> ,
27 1995 (Accessed, June 2006).
- 28 Hong, S.-Y., H-L Pan, Non Local Boundary Layer Vertical Diffusion in a Medium-Range
29 Forecast Model, *Monthly Weather Review*, 124, 2322-2339, 1996
- 30 Horowitz L. W., et al., A global simulation of tropospheric ozone and related tracers: Description
31 and evaluation of MOZART, version 2, *J. Geophys. Res.*, 108 (D24), 4784,
32 doi:10.1029/2002JD002853, 2003.
- 33 Jacob D. J., J. H. Crawford, M. M. Kleb, V. S. Connors, R. J. Bendura, J. L. Raper, G. W.
34 Sachse, J. C. Gille, L. Emmons, C. L. Heald, Transport and Chemical Evolution over the
35 Pacific (TRACE-P) aircraft mission: Design, execution, and first results, *J. Geophys.*
36 *Res.*, 108 (D20), 9000, doi:10.1029/2002JD003276, 2003.
- 37 Kiley C. M., et al., An intercomparison and evaluation of aircraft‐derived and simulated
38 CO from seven chemical transport models during the TRACE‐P experiment, *J.*
39 *Geophys. Res.*, 108 (D21), 8819, doi:10.1029/2002JD003089, 2003.
- 40 Kleinman, L., D. G. Daum, F. Brechtel, Y. Lee, J. Nunnermacker, S. Springton, J. Weinstein-
41 Lloyd, Efficiency of ozone production in the Houston plume, *American Meteorological*
42 *Society, Proceedings for Fourth Conference on Atmospheric Chemistry*,
43 http://ams.confex.com/ams/annual2002/techprogram/paper_32032.htm, 2002 (Accessed,
44 June 2006).
- 45 Kleinman, L. I., The dependence of tropospheric ozone production rate on ozone precursors,
46 *Atmospheric Environment*, 39, 575-586, 2005

- 1 Liao, D., D. Peuquet, Y. Duan, E. Whitsel, J. Dou, R. Smith, H-M. Lin, J-C. Chen, G. Heiss, GIS
2 approaches for the estimation of residential level ambient PM concentrations,
3 Environmental Health Perspectives, In press.
- 4 Mc Keen, S., J. Wilczak, G. Grell, S. Peckham, M. Pagowski, Real-time ozone forecasts over
5 Eastern North America during the summer of 2004: An assessment of several models and
6 their ensemble, Geophysical Research Abstracts, 7, 1-2, 2005
- 7 Parrish, D. D., Critical evaluation of US on-road vehicle emission inventories, Atmospheric
8 Environment, 40, 2288-2300, 2006
- 9 Pfister, G., P.G. Hess, L.K. Emmons, Lamarque, J-F., Wiedimeyer, C., Edwards, C.P., Petron,
10 G., Gille, J.C., Sachse, G.W., Quantifying CO emissions from the 2004 Alaskan wildfires
11 using MOPITT-CO data, Geophysical Research Letters, 32, 2005
- 12 Ramana, M. V., V. Ramanathan, I.A. Podgorny, B.B. Pradhan, B. Shrestha, The direct
13 observations of large aerosol radiative forcing in the Himalayan region, Geophysical
14 Research Letters 31, 2004
- 15 Singh, H. B., Brune, W., Crawford, J., Jacob, D., Overview of the summer 2004 Intercontinental
16 Chemical Transport Experiment-North America (INTEX-A), Journal Of Geophysical
17 Research-Atmospheres (This Issue)
- 18 Tang, Y., Carmichael, G.R., Uno, I. Woo, J., Kurata, G., Lefter, B., Shetter, R.E., Huang, H.,
19 Anderson, B.E., Avery, M.A., Clarke, A.D., Blake, D.R., Impacts of aerosols and clouds
20 on photolysis frequencies and photochemistry during TRACE-P, part II: three-
21 dimensional study using a regional chemical transport model, Journal Of Geophysical
22 Research-Atmospheres. 108 (D21), 8822, doi:10.1029/2002JD003100, 2003
- 23 Tang, Y., G.R. Carmichael, D. Seinfeld, R.W. Dabdub, B. Huebert, A.D. Clarke, S.A. Guazzotti,
24 D.A. Sodeman, K.A. Prather, I. Uno, J-H. Woo, D.G. Streets, P.K. Quinn, Three-
25 dimensional simulations of inorganic aerosol distributions in East Asia during spring
26 2001, Journal Of Geophysical Research-Atmosphere, 109, D19S23,
27 doi:10.1029/2003JD004201, 2004
- 28 Tang, Y., G.R. Carmichael, N. Thongbonchoo, T. Chai, L.W. Horowitz, R. Pierce, J.A. Al-Saadi,
29 G. Pfister, J. Vukovich, M. Avery, G.W. Sachse, T.B. Ryerson, J.S. Holloway, E.
30 Atlas, F. Flocke, R. Weber, G. Huey, J. Dibb, D.G. Streets, W. Brune, The Influence of
31 Lateral and Top Boundary Conditions on Regional Air Quality Prediction: a multi-scale
32 study coupling regional and global chemical transport models., Journal Of Geophysical
33 Research-Atmosphere, This Issue.
- 34 Trainer, M., D. D. Parrish, M. P. Buhr, R. B. Norton, F. C. Fehsenfeld, K. G. Anlauf, J. W.
35 Bottenheim, Y. Z. Tang, H. A. Wiebe, J. M. Roberts, R. L. Tanner, L. Newman, V. C.
36 Bowersox, J. F. Meagher, K. J. Olszyna, M. O. Rodgers, T. Wang, H. Berresheim, K. L.
37 Demerjian, U. K. Roychowdhury, Correlation of ozone within NO_y in photochemically
38 aged air, J. Geophys. Res., 98(D2), 2917-2925, 10.1029/92JD01910, 1993.
- 39

Table 1 Total column emissions in model domain, in Tg/year, including point source, area, and aviation emissions. CO emissions reported as Tg C/year, and NO_x emissions as Tg N/year.

	Emissions (Tg/year)	
	CO	NO _x
NEI 1999	40.7	7.1
NEI 2001	25.0	5.2
NEI 2001-Frost LPS	26.8	4.8
NEI 2001-Frost LPS-Modified	26.8	4.2

Table 2 Summary of model parameters for different scenarios.

	Model specifications and comments
Forecast	1999 National Emissions Inventory, BEIS2 Biogenic Emissions, biomass burning input through forecasted boundary conditions from MOZARTT-GFDL using climatological fires. Underpredicted NO _x and O ₃ dry deposition due to dormant agricultural lands. No lightning NO _x emissions. MM5 forecast from AVN global model.
NEI2001-FrostLPS	2001 National Emissions Inventory, Frost updated 2004 Large Point Sources, BEIS2 Biogenic emissions, biomass burning input through boundary conditions through MOZARTT-NCAR [Pfister <i>et al.</i> , 2005]. Upper troposphere lightning NO _x emissions. MM5 prediction through FNL reanalysis. Dry deposition corrected for summer season. VOC adjustments for alkanes and aromatics.
NEI2001-FrostLPS-Modified	Same as before, but modifying Area NO _x emissions by a factor of 0.4 for Alabama, Mississippi, Georgia, North Carolina, South Carolina, Tennessee, West Virginia, Indiana, and Ohio.

Table 3 Model performance statistics for selected species. Modeled vs. Observed data, DC-8 Platform.0-12km range. Frost LPS: NEI2001-FrostLPS. Frost LPS*: NEI2001-Frost LPS-Modified.

	O₃			CO			NO_y		
	Forecast	Frost-LPS	FrostLPS*	Forecast	Frost-LPS	FrostLPS*	Forecast	Frost-LPS	FrostLPS*
	0-1km								
R	0.71	0.70	0.72	0.61	0.68	0.65	0.66	0.59	0.56
Mean observed (ppbv)	48.92	48.92	48.92	138.08	138.08	138.08	1.84	1.84	1.84
Mean modeled (ppbv)	60.12	51.82	50.36	151.33	136.60	139.27	4.36	3.10	2.95
S.D./Mean observed	0.36	0.36	0.33	0.28	0.28	0.27	1.00	1.00	0.95
S.D./Mean modeled	0.39	0.34	0.33	0.36	0.29	0.27	0.79	0.70	0.67
mean bias (ppbv)	11.21	2.90	1.45	9.75	-2.48	-1.35	2.70	1.40	1.11
	1-4km								
R	0.40	0.48	0.50	0.49	0.65	0.65	0.40	0.48	0.50
Mean observed (ppbv)	57.34	57.34	57.34	119.43	119.43	119.43	57.34	57.34	57.34
Mean modeled (ppbv)	59.04	54.74	53.32	131.93	125.14	125.25	59.04	54.74	53.32
S.D./Mean observed	0.22	0.22	0.20	0.26	0.26	0.26	0.22	0.22	0.20
S.D./Mean modeled	0.32	0.26	0.25	0.33	0.25	0.26	0.32	0.26	0.25
mean bias (ppbv)	1.63	-2.66	-4.02	11.37	5.20	5.82	1.63	-2.66	-4.02

*Modified area NO_x emissions, SD: Standard deviation

Table 3 (Continued) Model performance statistics for selected species. Modeled vs. Observed data, DC-8 Platform.0-12km range. Frost LPS: NEI2001-FrostLPS. Frost LPS*: NEI2001-Frost LPS-Modified.

	O₃			CO			NO_y		
	Forecast	Frost-LPS	FrostLPS*	Forecast	Frost-LPS	FrostLPS*	Forecast	Frost-LPS	FrostLPS*
	4-8km								
R	0.40	0.38	0.39	0.01	0.45	0.45	0.03	0.15	0.15
Mean observed (ppbv)	68.69	68.69	68.69	99.36	99.36	99.36	0.72	0.72	0.72
Mean modeled (ppbv)	53.11	59.84	59.69	85.63	93.53	92.12	0.51	1.19	1.19
S.D./Mean observed	0.25	0.25	0.25	0.40	0.40	0.19	0.55	0.55	0.54
S.D./Mean modeled	0.19	0.18	0.18	0.17	0.18	0.15	0.64	1.09	1.05
Mean bias (ppbv)	-15.59	-8.85	-9.00	-14.13	-7.32	-7.25	-0.21	0.47	0.47
	8-12-km								
R	0.52	0.42	0.42	0.05	0.20	0.20	0.11	0.05	0.05
Mean observed (ppbv)	92.69	92.69	92.69	96.36	96.36	96.36	1.28	1.28	1.28
Mean modeled (ppbv)	75.25	76.83	76.82	72.02	77.59	77.86	0.40	1.64	1.67
S.D.*/Mean observed	0.54	0.54	0.56	0.25	0.25	0.22	0.57	0.57	0.54
S.D.*/Mean modeled	0.35	0.15	0.15	0.11	0.14	0.14	0.31	2.17	2.25
Mean bias (ppbv)	-17.45	-15.86	-15.87	-25.12	-18.51	-18.50	-0.89	0.38	0.38

*Modified area NO_x emissions, SD: Standard deviation

Table 4 Model performance statistics for selected species. Modeled vs Observed data, P-3 Platform.0-12km range. Frost LPS: NEI2001-FrostLPS. Frost LPS*: NEI2001-Frost LPS-Modified.

	O₃			CO			NO_y		
	Forecast	Frost-LPS	FrostLPS*	Forecast	Frost-LPS	FrostLPS*	Forecast	Frost-LPS	FrostLPS*
R Mean observed (ppbv) Mean modeled (ppbv) S.D./Mean observed S.D./Mean modeled mean bias (ppbv)	0-1km								
	0.63	0.66	0.69	0.43	0.42	0.42	0.28	0.29	0.29
	56.27	56.27	56.27	158.60	158.60	158.60	3.91	3.91	3.91
	64.52	57.60	55.93	202.81	163.56	164.49	7.77	5.03	4.79
	0.35	0.35	0.35	0.24	0.24	0.24	0.72	0.72	0.72
	0.38	0.31	0.30	0.31	0.24	0.24	0.65	0.63	0.65
	8.26	1.34	-0.34	44.24	4.96	5.89	3.87	1.12	0.88
R Mean observed (ppbv) Mean modeled (ppbv) S.D./Mean observed S.D./Mean modeled mean bias (ppbv)	1-4km								
	0.57	0.63	0.65	0.52	0.66	0.66	0.64	0.64	0.65
	60.16	60.16	60.16	135.66	135.66	135.66	2.38	2.38	2.38
	65.07	62.05	59.59	164.04	143.34	144.46	5.00	3.58	3.34
	0.23	0.23	0.23	0.34	0.34	0.34	0.88	0.88	0.88
	0.34	0.27	0.26	0.38	0.28	0.28	0.86	0.71	0.73
	4.91	1.89	-0.58	28.37	7.67	8.79	2.62	1.20	0.96

SD: Standard deviation

Table 4 (Continued) Model performance statistics for selected species. Modeled vs Observed data, P-3 Platform.0-12km range. Frost LPS: NEI2001-FrostLPS. Frost LPS*: NEI2001-Frost LPS-Modified.

	O₃			CO			NO_y		
	Forecast	Frost-LPS	FrostLPS*	Forecast	Frost-LPS	FrostLPS*	Forecast	Frost-LPS	FrostLPS*
	4-8km								
R	0.15	0.44	0.46	0.11	0.36	0.36	0.24	0.40	0.39
Mean observed (ppbv)	66.80	66.80	66.80	106.66	106.66	106.66	1.13	1.13	1.13
Mean modeled (ppbv)	50.61	59.74	58.97	92.08	101.37	101.77	0.82	1.34	1.29
S.D./Mean observed	0.16	0.16	0.16	0.33	0.33	0.33	0.35	0.35	0.35
S.D./Mean modeled	0.14	0.20	0.19	0.13	0.24	0.24	0.67	0.62	0.64
mean bias (ppbv)	-16.19	-7.06	-7.83	-14.57	-5.28	-4.88	-0.31	0.21	0.16

SD: Standard deviation

Table 5 Comparison of correlation coefficients of observed ozone and ozone bias to selected species, at different altitude ranges, for DC-8 platform. Bias calculated with respect to NEI2001-FrostLPS. Ranges 0-1km, 1-4km, 4-8km, 8-12km

	Observation Correlation Coefficients				Bias Correlation Coefficients.			
	0-1km	1-4km	4-8km	8-12km	0-1km	1-4km	4-8km	8-12km
Acetone	0.68	0.21	0.11	-0.12	0.42	0.15	0.10	-0.14
ARO2	-0.02	0.11	0.31		0.04	0.04	0.89 (n=6)	-0.95
ARO1	0.47	0.40	0.01	0.07	0.09	0.07	0.13	0.02
Acetaldehyde	0.38	-0.07	0.04	0.10	0.24	0.20	-0.07	0.12
CO	0.70	0.44	0.08	-0.24	0.51	0.44	0.19	-0.32
Ethene	0.24	0.06	-0.04	-0.07	0.04	-0.05	0.02	-0.05
Ethyne	0.75	0.48	0.14	0.00	0.18	0.25	0.26	-0.07
H ₂ O ₂	0.51	0.24	-0.29	-0.28	0.28	-0.01	-0.27	-0.29
Formaldehyde	0.53	0.07	-0.09	-0.12	0.20	0.11	0.18	-0.04
HNO ₃	0.86	0.50	0.19	0.67	0.47	0.45	0.44	0.36
HO ₂	0.48	0.23	-0.14	-0.28	0.15	0.09	0.14	-0.10
Isoprene	-0.03	-0.03	-0.19		-0.48	-0.38	-0.34	
MEK	0.04	0.06	-0.03	-0.17	0.48	0.44	0.11	-0.03
NO	0.04	0.04	-0.07	-0.23	-0.17	0.07	0.10	0.04
NO ₂	0.05	0.10	0.02	-0.08	-0.07	0.20	0.20	0.10
NO _y	0.04	0.02	-0.08	-0.24	0.34	0.55	0.39	0.10
NO _z	0.65	0.17	0.08	-0.14	0.45	0.57	0.50	0.28
OH	0.58	0.20	0.12	-0.18	0.24	0.23	-0.09	-0.01
PAN	-0.03	-0.06	0.19	-0.04	0.60	0.64	0.43	-0.05
Propane	0.15	0.07	0.48	0.14	0.14	0.14	0.01	-0.10
Propene	0.63	0.30	0.48	0.27	-0.25	-0.12	0.13	
RH	0.77	0.37	0.47	0.42	-0.14	-0.05	-0.03	-0.08
SO ₂	0.55	0.24	0.23	0.12	0.07	0.35	0.17	-0.01
Temperature	0.64	0.46	0.39	0.03	0.27	0.15	-0.08	-0.41
Wind Speed	0.40	0.16	0.06	-0.10	0.04	0.10	0.09	0.06

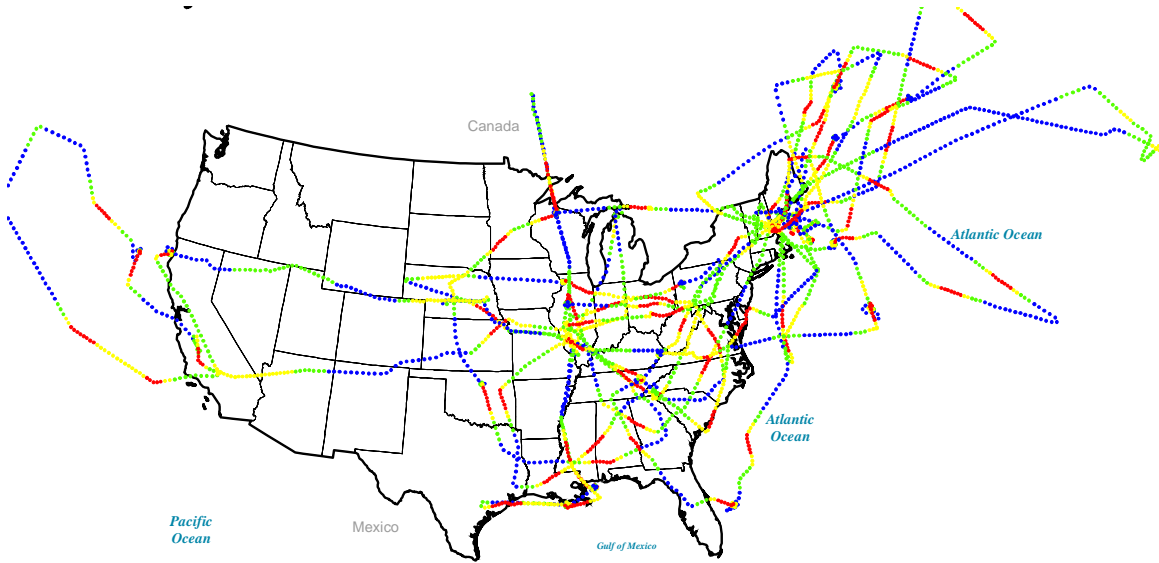


Figure 1 DC-8 flight tracks and altitude range for the INTEX-A portion of ICARTT. In red: 0-1km, Yellow: 1-4km, Green: 4-8km, Blue: 8-12km.

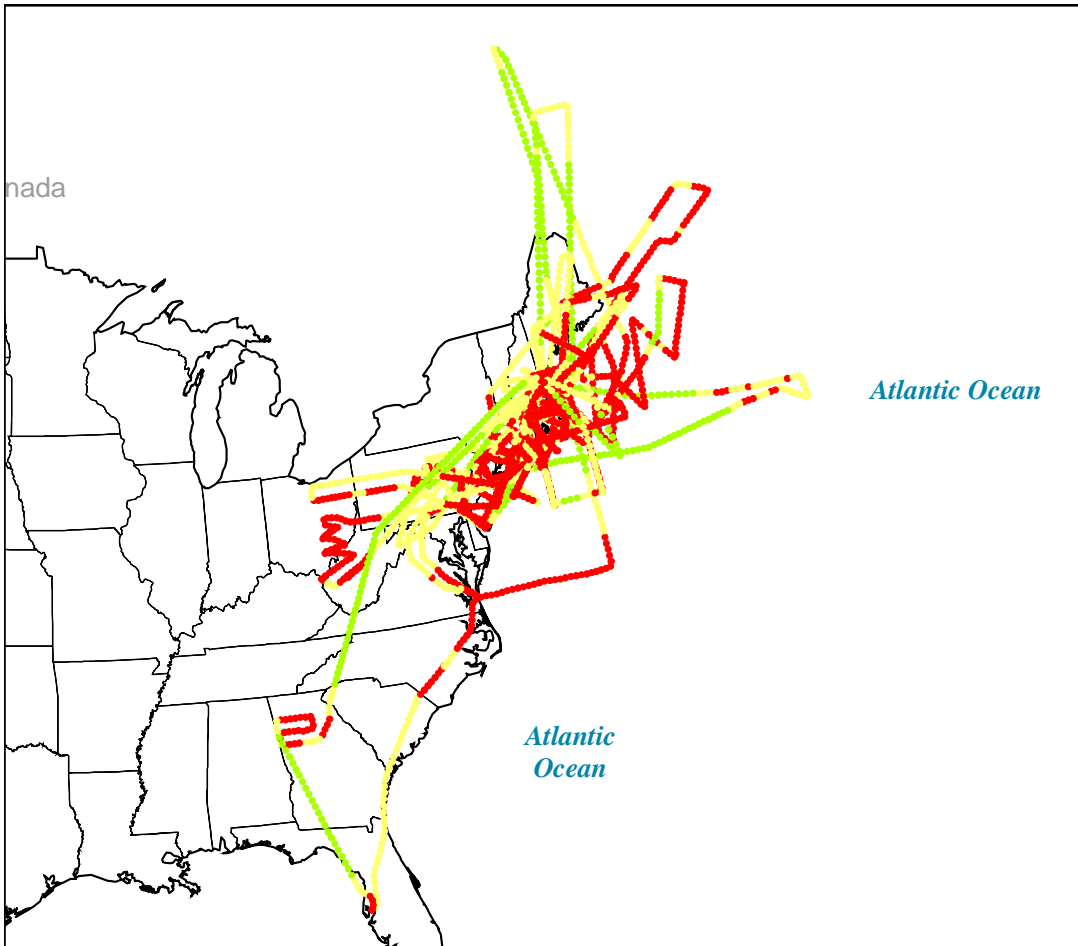


Figure 2 P-3 flight tracks and altitude range for NEAQS2K-4 portion of ICARTT, colored by altitude. In Red: 0-1km, Yellow: 1-4km, Green: 4-8km

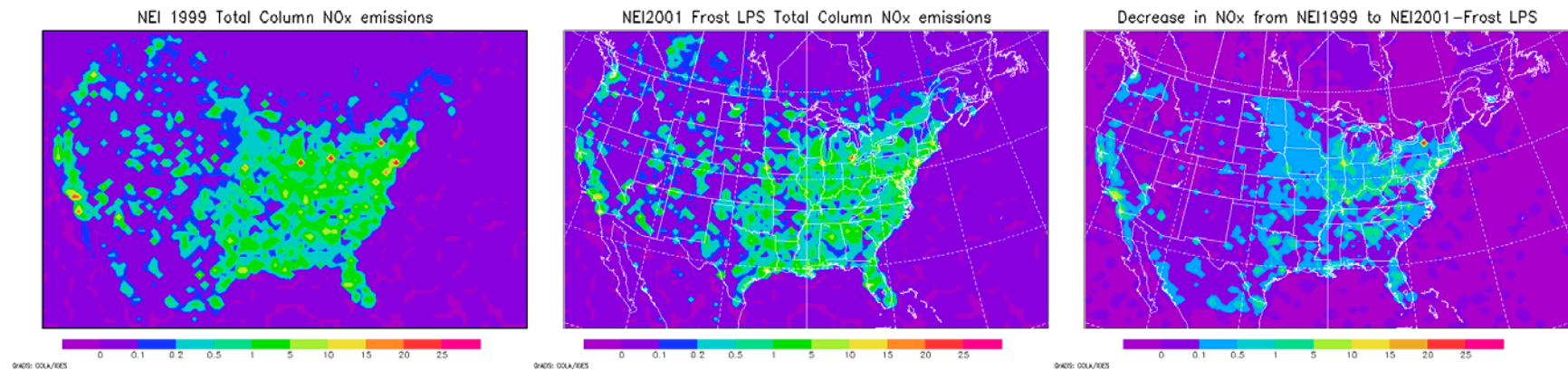
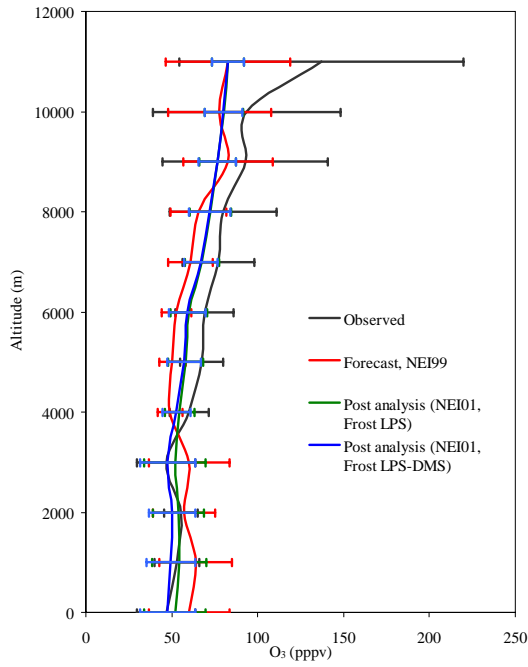
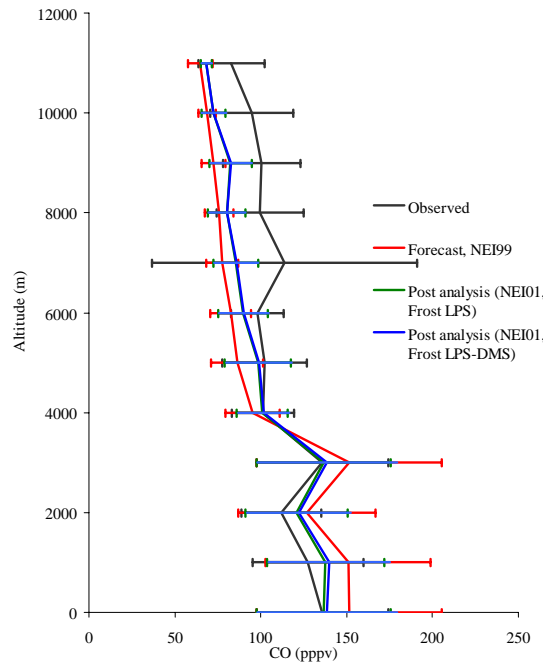


Figure 3 Total Column NO_x emissions Left: NEI 1999. Center NEI 2001-Frost LPS emissions. Right: Decrease in NO_x emissions from NEI 1999 to NEI 2001- Frost LPS. Scale in tonnes/km²/year.

A.)



B.)



C.)

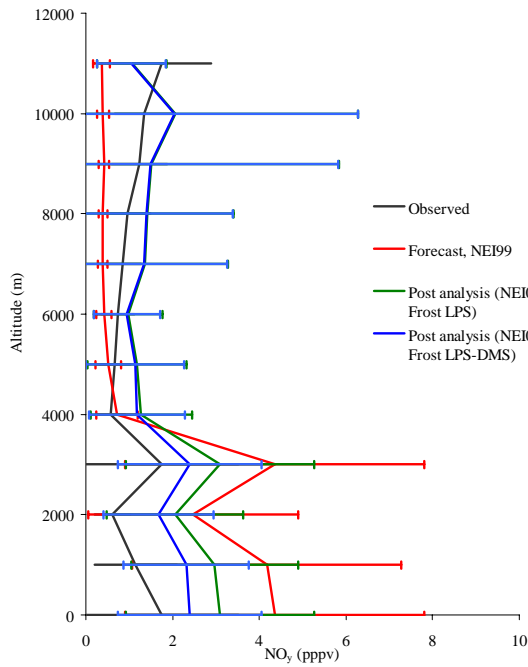


Figure 4 Observed and 60km-simulated O₃, CO, NO_y, and HNO₃ profiles and standard deviations for all DC-8 flights. A.) Ozone. B.) CO C.) NO_y. Blue: NEI 2001-Frost LPS-Modified. Red: Forecast, NEI 1999. Black: Observed.

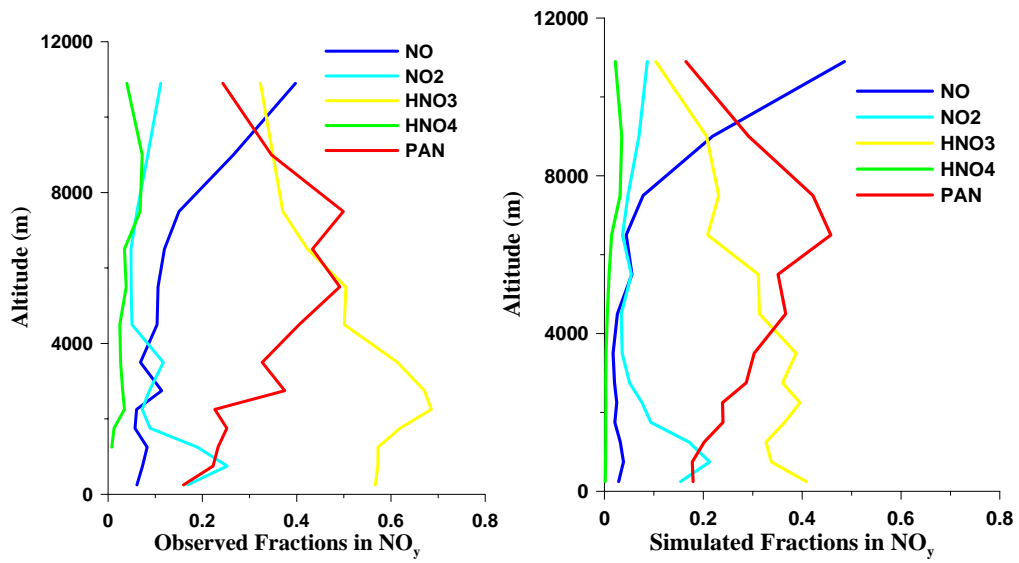


Figure 5. Comparison of mean contributions to NO_y along the DC8 flight tracks as a function of altitude. Left- observed values; Right-predicted for the NEI2001-Frost-LPS case. Values are plotted as fraction of total NO_y.

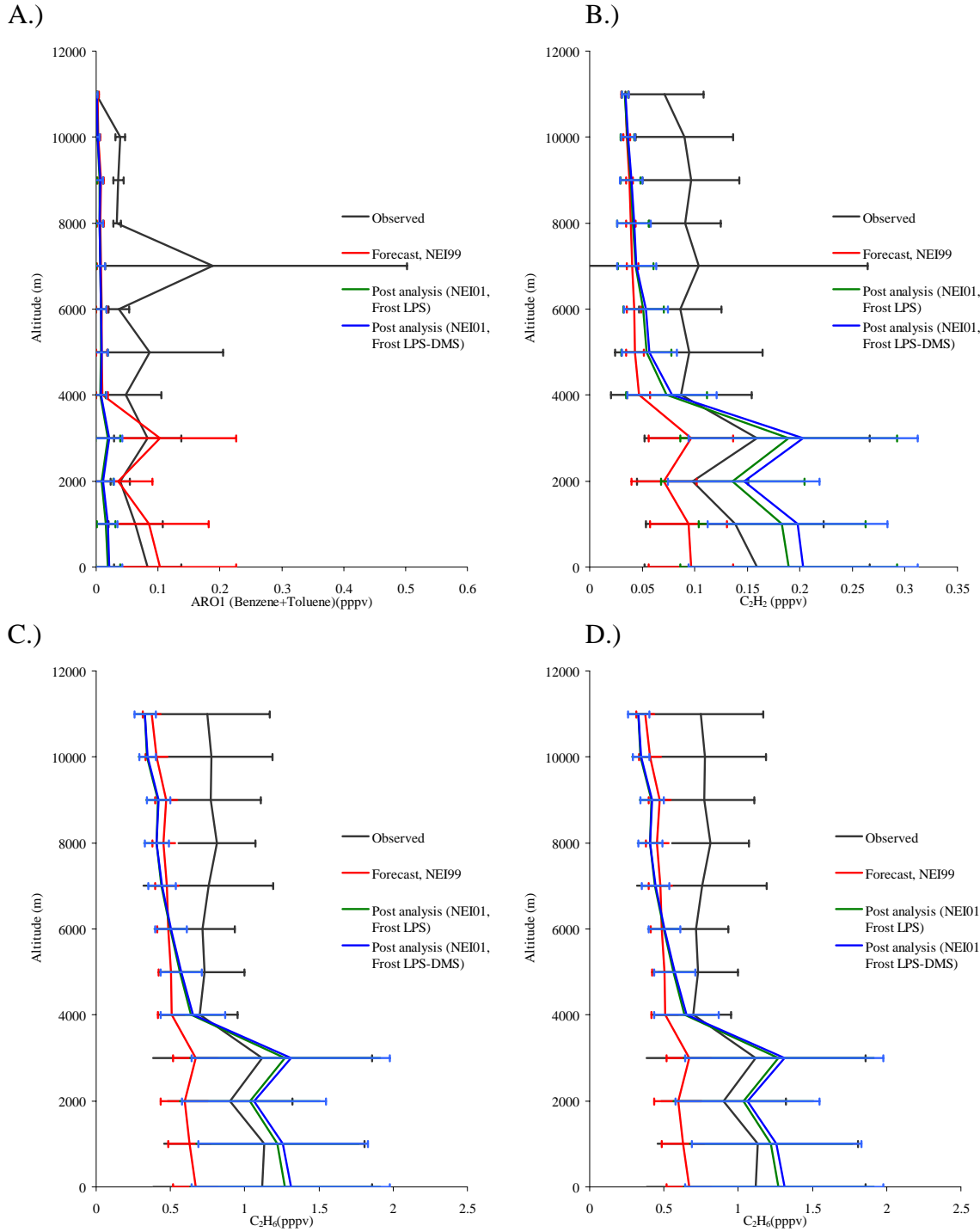


Figure 6 Observed and 60km-simulated A.) ARO1, B.) C₂H₂, C.) C₂H₆, and D.) C₃H₈ profiles and standard deviations for all DC-8 flights.

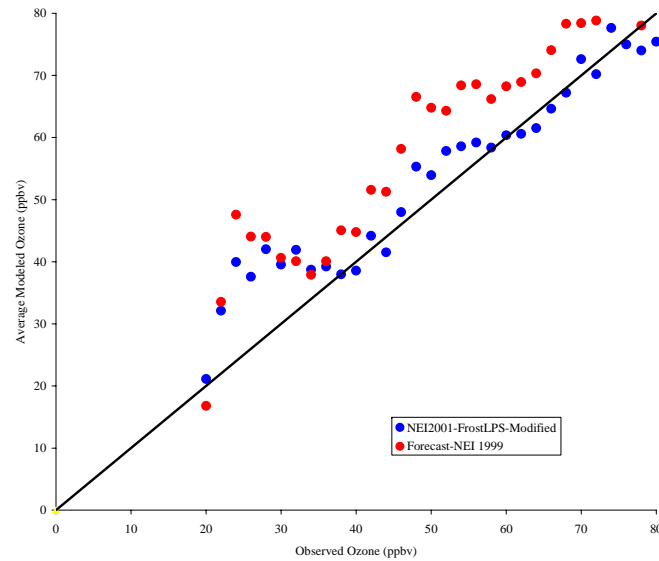
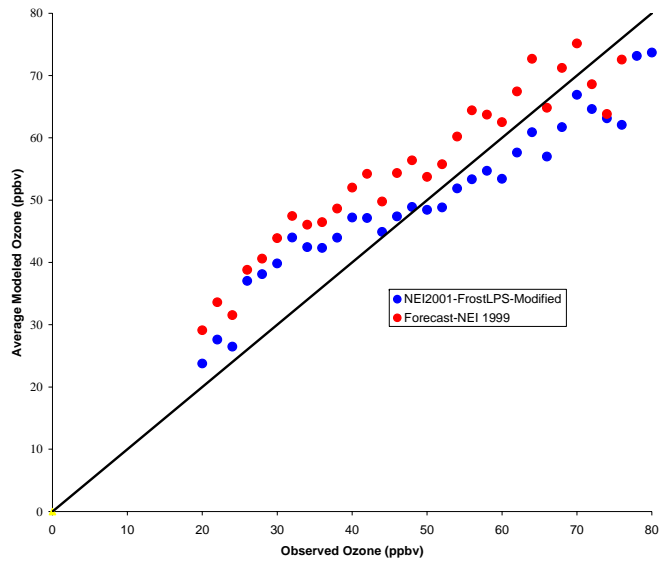


Figure 7 Quantile-quantile plots of modeled ozone with observed ozone for Left: DC-8 platform Right: WP-3, for data points collected at altitude less than 4000m, STEM-2k4, Forecast: NEI 1999, Post Analysis: NEI2001-Frost LPS-Modified. MOZART-NCAR boundary conditions.

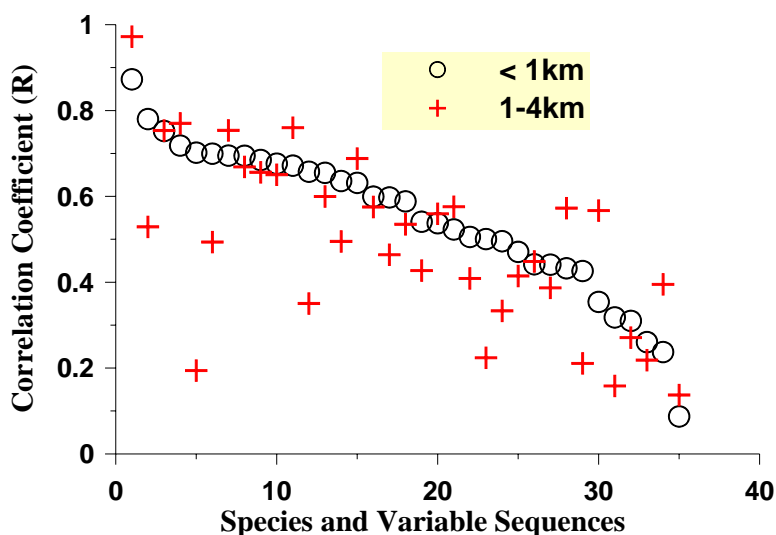


Figure 8 Correlation coefficients for all INTEX-A DC-8 flights (NEI2001-Frost LPS, MOZART NCAR B.C.), 60km resolution. Species list are:

1	Temperature ($^{\circ}$ K)	13	HNO ₃	25	HO ₂
2	SO ₄ ²⁻ Filter	14	PAN	26	CH ₃ CHO
3	Wind Speed (m/s)	15	Relative Humidity	27	NO
4	HCHO NCAR	16	NO _z	28	Propane
5	Submicron Aerosol Absorption (/m) @550nm	17	OH	29	Ethene
6	O ₃	18	NO _y	30	RNO ₃
7	J[O ₃ => O ₂ + O ¹ D]	19	H ₂ O ₂	31	C8+ Aromatics
8	SO ₄ ²⁻ PILS	20	J[NO ₂]	32	Ethyne
9	HNO ₃ + Nitrate	21	SO ₂	33	Benzene + Toluene
10	CO	22	NO _x	34	Ethane
11	J[Acetone]	23	Acetone	35	Liquid Water Content (g/m ³)
12	Isoprene	24	NO ₂		

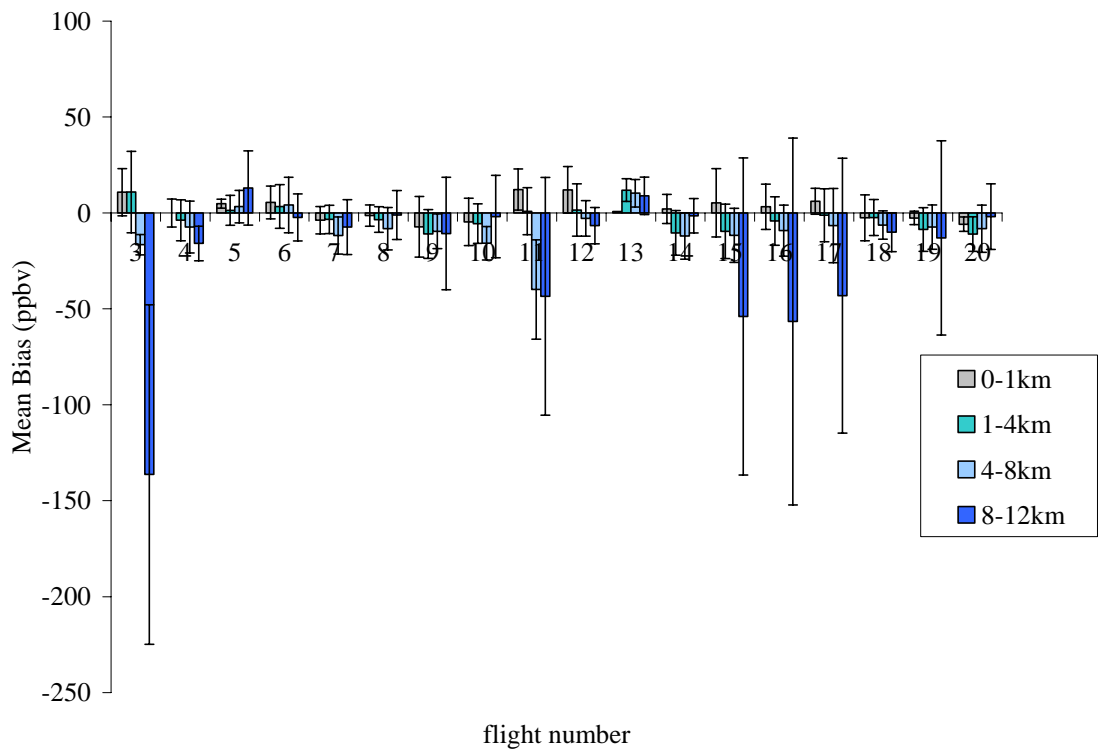


Figure 9 Mean ozone bias for DC-8 flights 3-20, separated by altitude range. NEI2001-FrostLPS-DMS case. Error bars represent standard deviation.

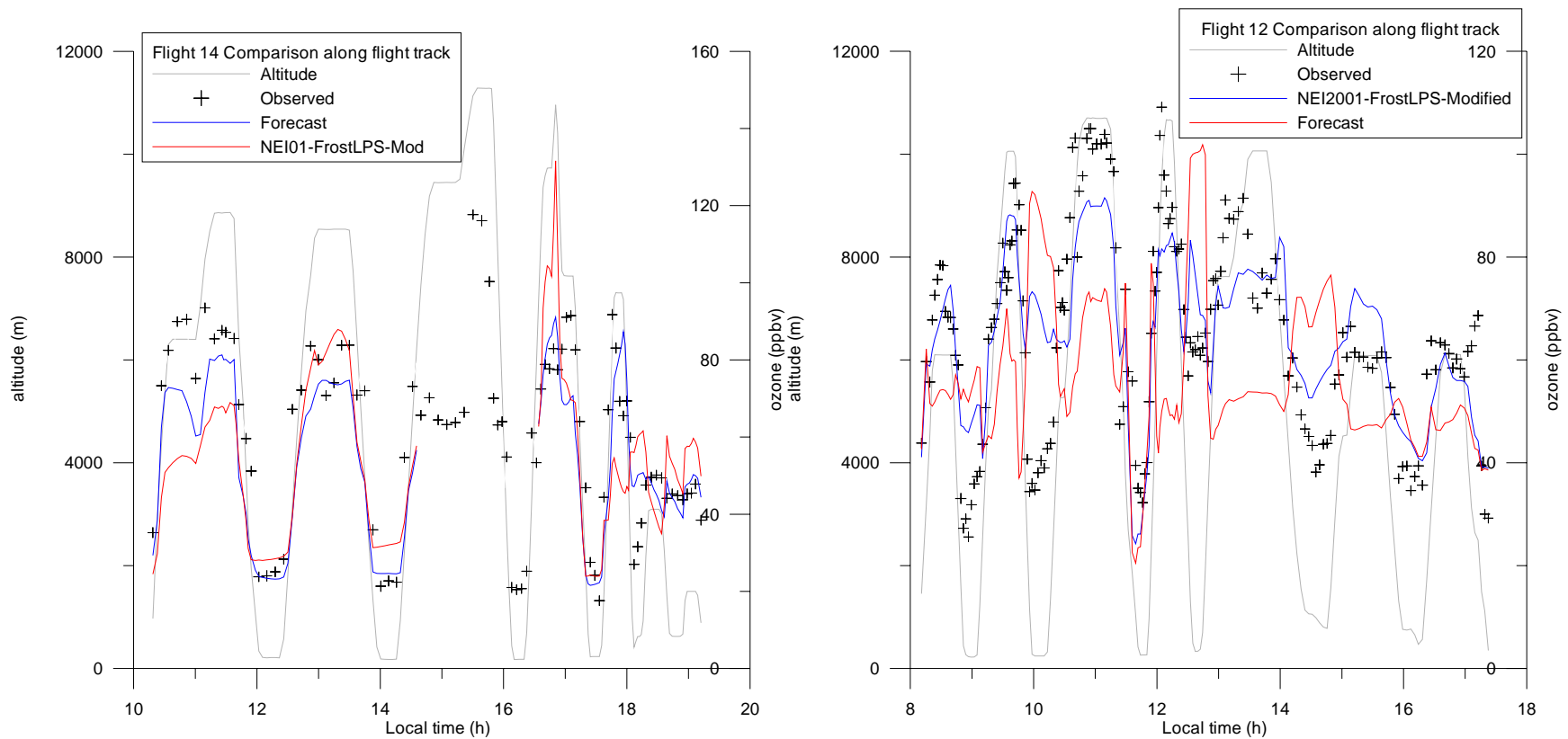


Figure 10 Left: Time series of observed and modeled ozone along DC-8 Flight 14 flight track (July 31, 2004). Absence of modeled data denotes that flight went beyond model boundaries. Forecast: $n=142$, $R=0.65$, Bias (0-1km) = 8.10 ppb, Bias (8-12km) = 5.14 ppb. NEI2001-Frost-Modified: $n=142$, $R=0.84$, Bias (0-1km) = 2.05 ppb, Bias (8-12km) = -1.47 ppb. Right: Time series of observed and modeled ozone along DC-8 Flight 12 track (July 25, 2004). Absence of modeled data denotes that flight went beyond model boundaries. Forecast: $n=185$, $R=0.01$, Bias (0-1km) = 22.84 ppb, Bias (8-12km) = -30.51 ppb. NEI2001-Frost-Modified: $n=185$, $R=0.78$, Bias (0-1km) = 12.02 ppb, Bias (8-12km) = 6.6 ppb

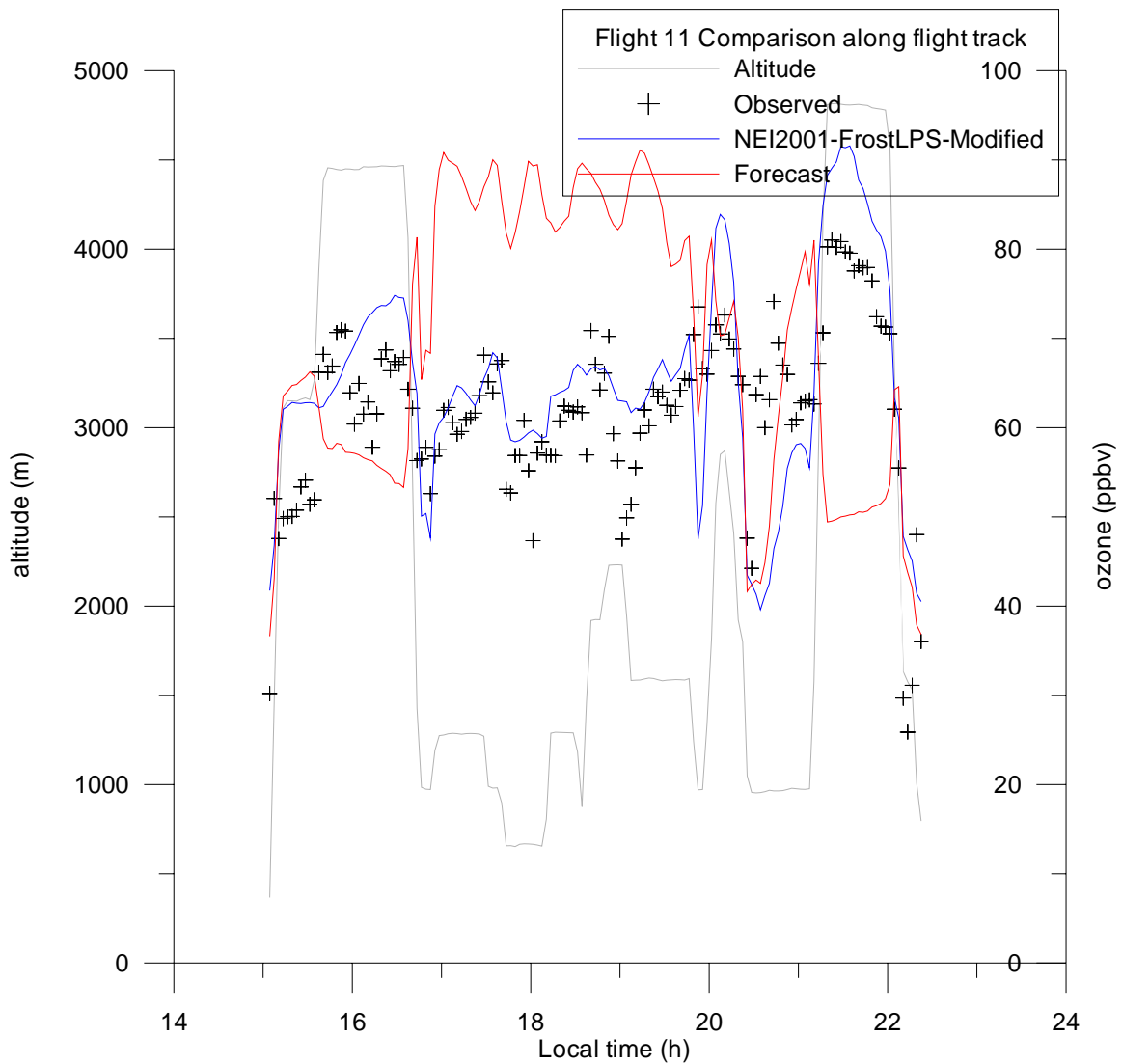


Figure 11 Time series of observed and modeled ozone along WP-3 Flight 11 track (July 27, 2004). Forecast, $n=157$, $R=-0.02$, Bias (0-4km) =15.46 ppb Bias (4-5km) = -16.63 ppbv. NEI2001-Frost-Modified, $n=157$, $R=0.67$. Bias (0-4km) =1.41 ppbv, Bias (4-5km) =6.6 ppbv

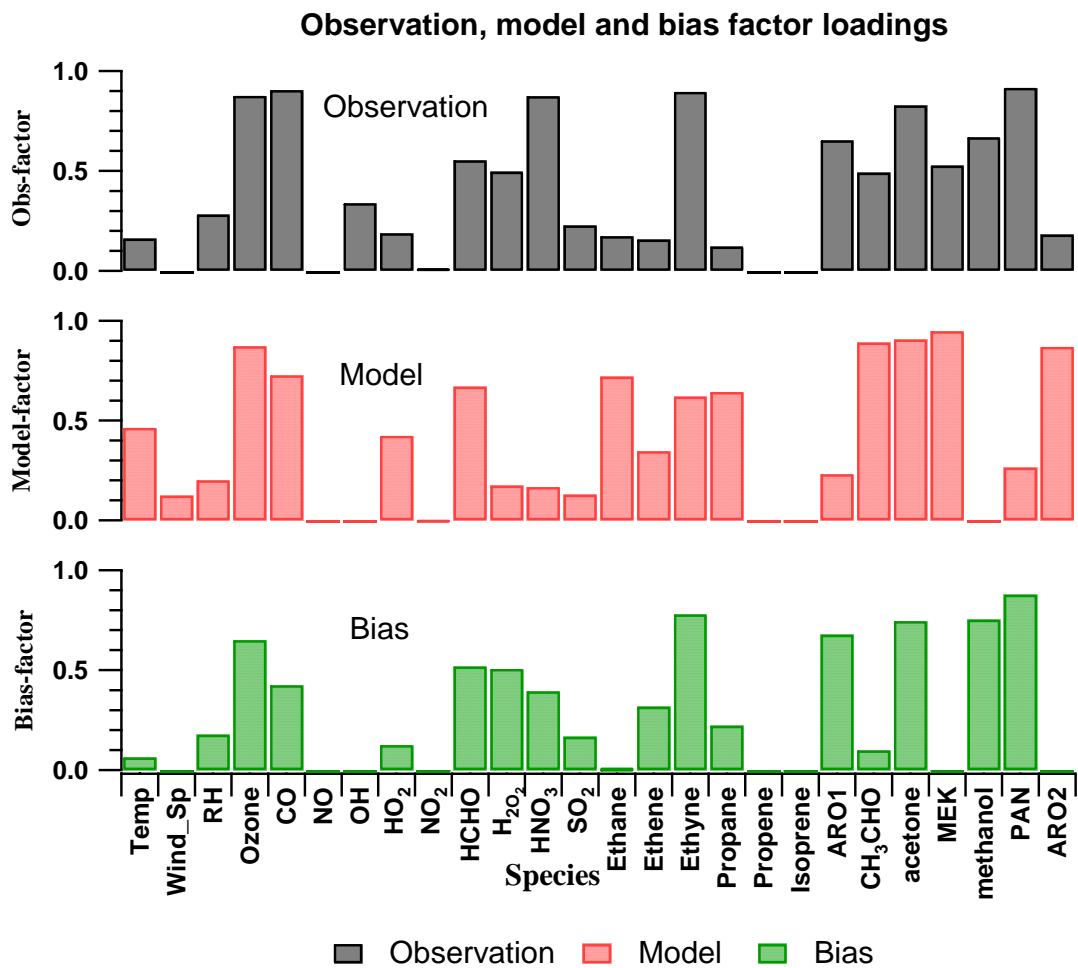


Figure 12 Factor analyses for DC-8, points in 0-1km range. Top: Observations. Center: Model. Bottom: Bias of model with respect to observations. Factor criteria of 90% variance.

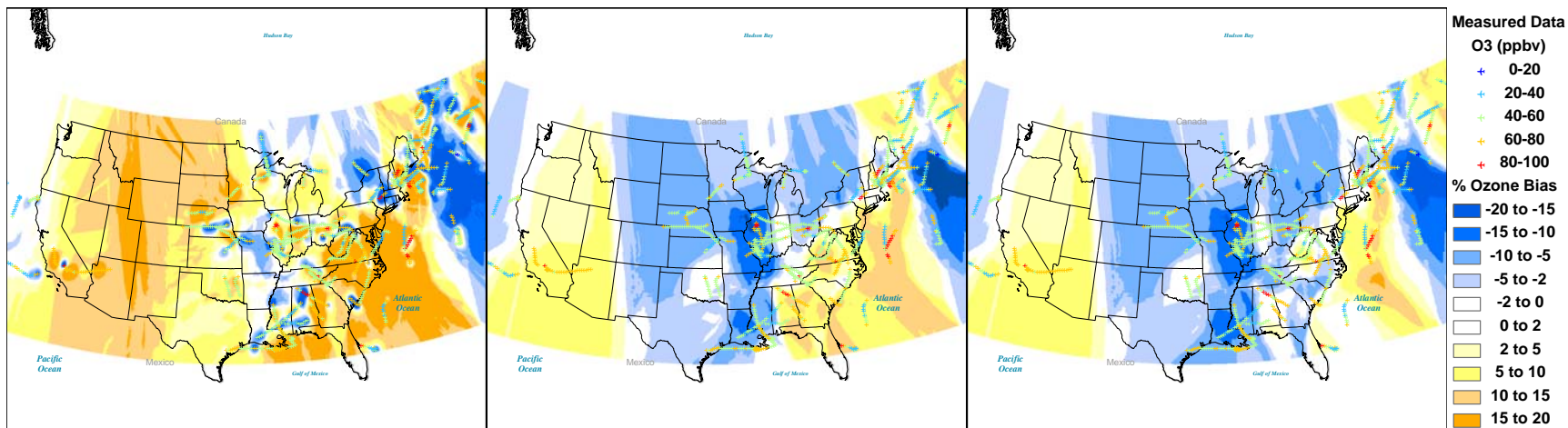


Figure 13 Kriged ozone percent bias (modeled-observed) for alt<4000m, DC-8 platform, n=1208, Left: Forecast, NEI 1999 Center: NEI 2001, Frost LPS. Right: NEI 2001, Frost LPS-Modified

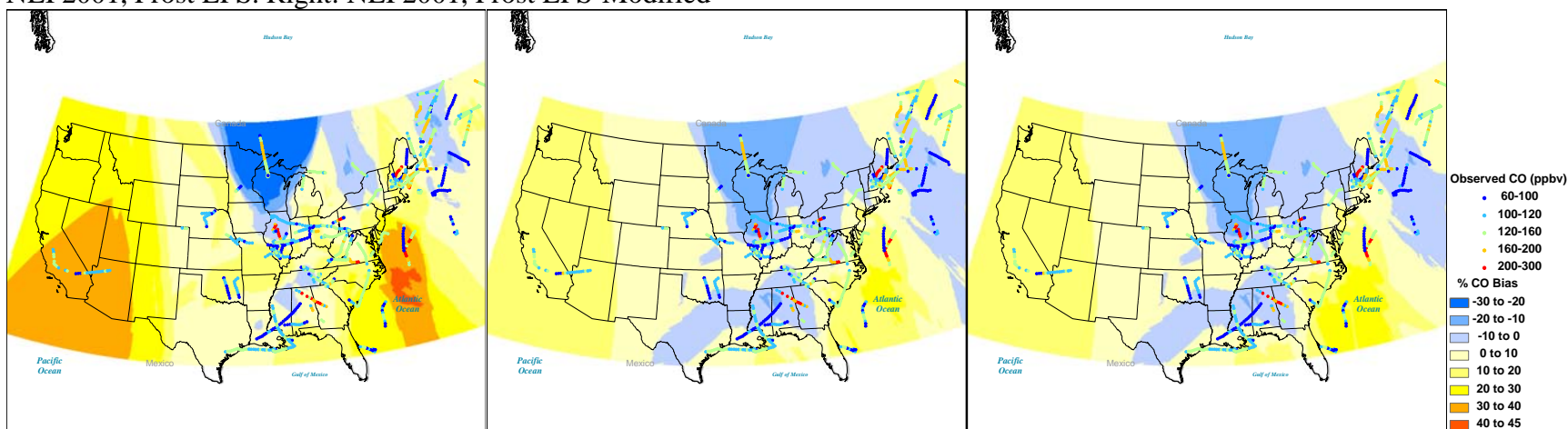


Figure 14 Kriged CO percent bias (modeled-observed) for alt<4000m, DC-8 platform, n=1002, Left: Forecast, NEI 1999 Center: NEI 2001, Frost LPS. Right: NEI 2001, Frost LPS-Modified

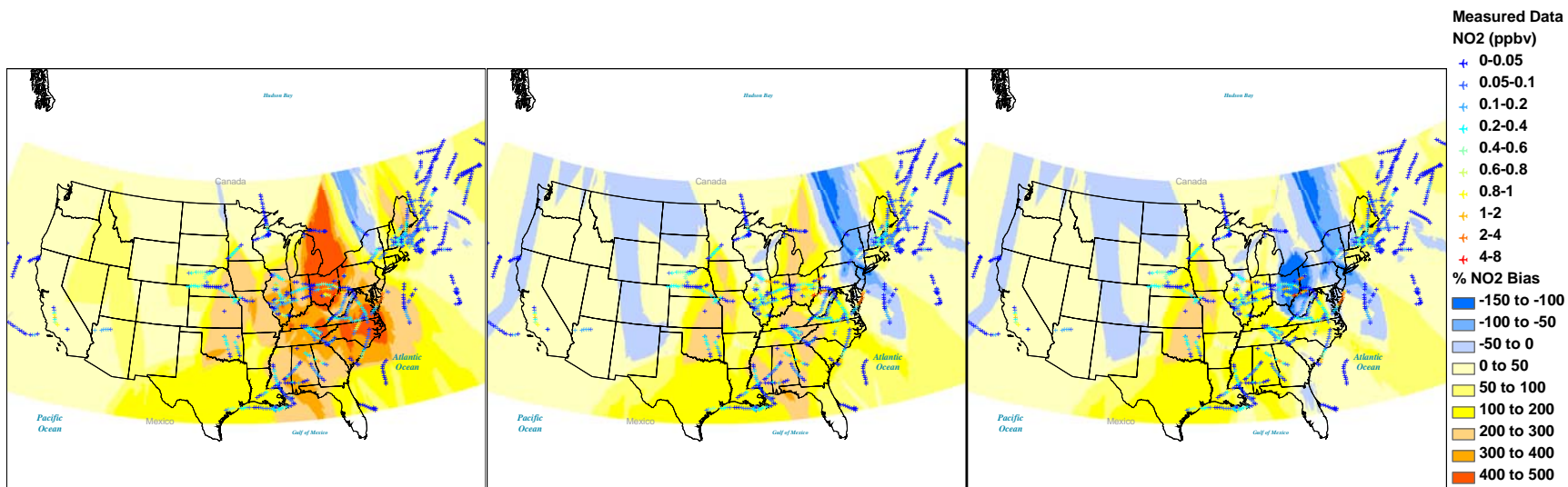


Figure 15 Kriged NO₂ percent bias (modeled-observed) for alt<4000m, DC-8 platform, n=1080, Left: Forecast, NEI 1999 Center: NEI 2001, Frost LPS. Right: NEI 2001, Frost LPS-Modified

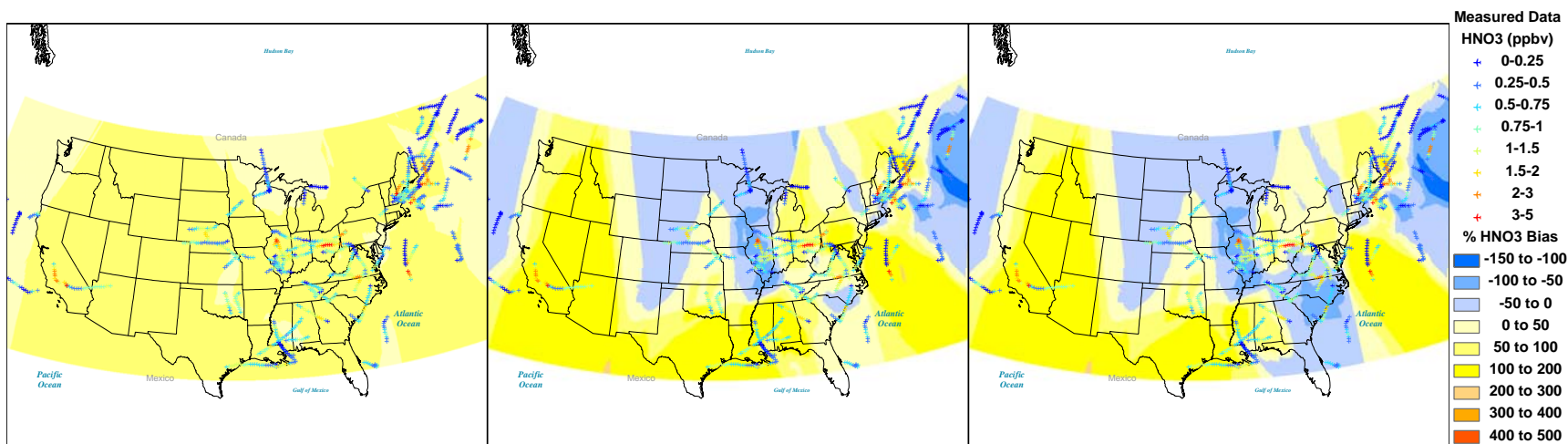


Figure 16 Kriged HNO₃ percent bias (modeled-observed) for alt<4000m, DC-8 platform, n=1158, Left: Forecast, NEI 1999 Center: NEI 2001, Frost LPS. Right: NEI 2001, Frost LPS-Modified

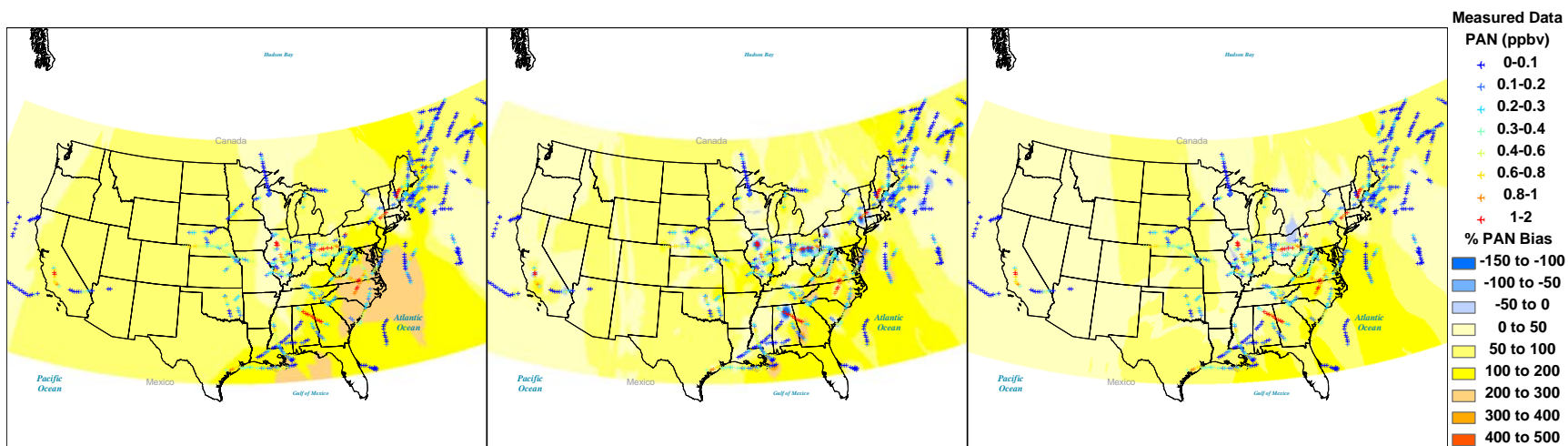


Figure 17 Kriged PAN percent bias (modeled-observed) for alt<4000m, DC-8 platform, n=976, Left: Forecast, NEI 1999 Center: NEI 2001, Frost LPS. Right: NEI 2001, Frost LPS-Modified

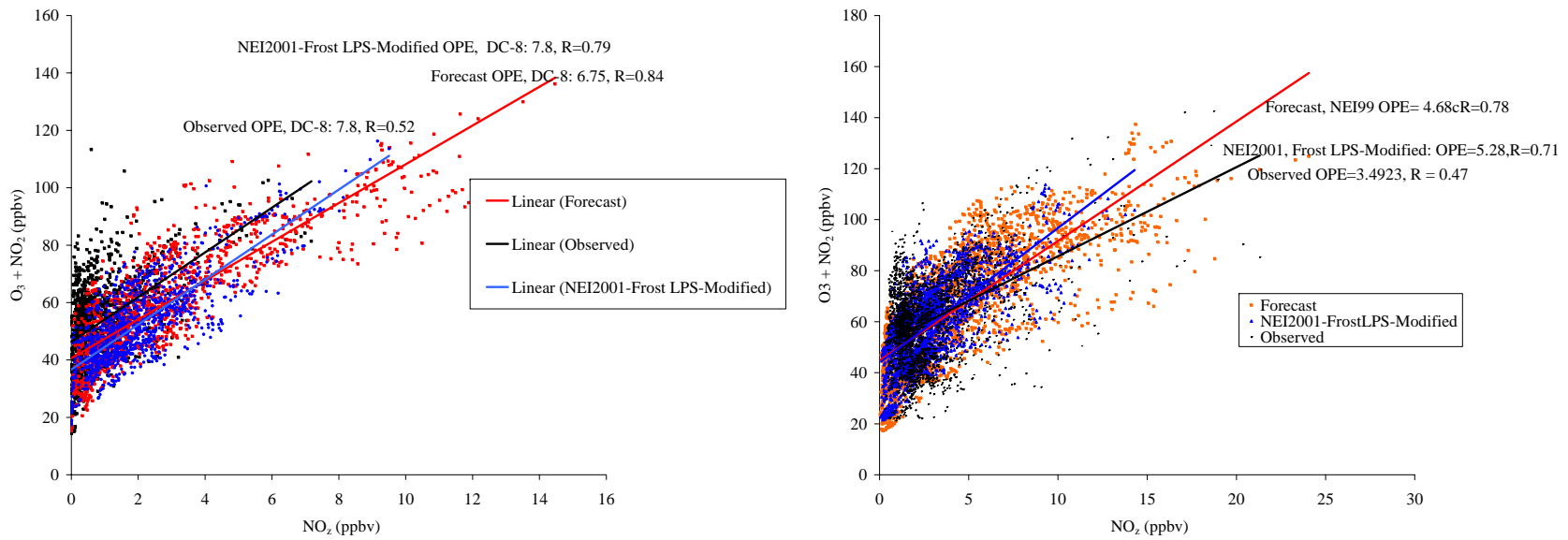


Figure 18 Observed and Modeled Ozone Production Efficiency (OPE). Left: DC-8. Right: WP-3 for data points with altitude < 4000m, all flights. Red: Forecast, NEI 1999. Blue: NEI 2001-Frost LPS-Modified.

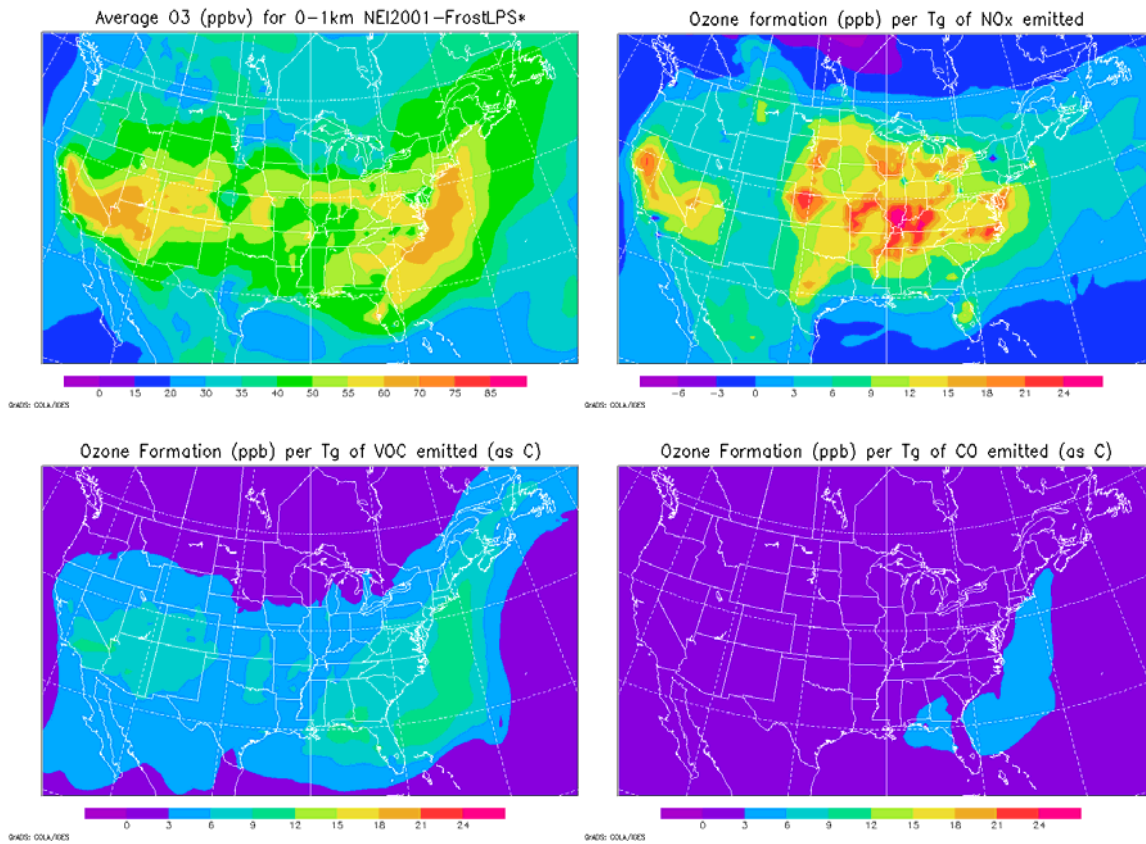
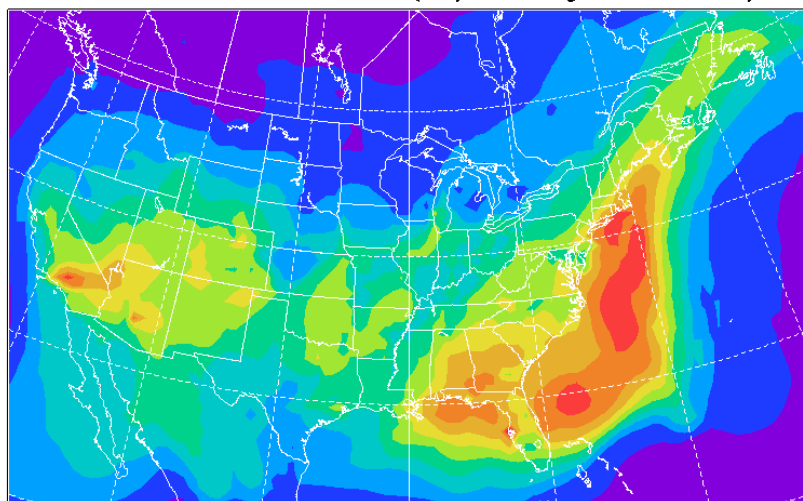


Figure 19 Top Left: Modeled near surface ozone (0-1km average) for NEI-2001-FrostLPS-Modified case. Modeled ozone formation (ppbv) per Tg of precursor emitted: Top Right: NO_x, Bottom Left: Anthropogenic VOC emissions. Bottom Right: Anthropogenic CO. July 21 to August 16, 2004.

VOC contribution to Ozone (July 21–August 18, 2004)



CO contribution to Ozone (July 21–August 18, 2004)

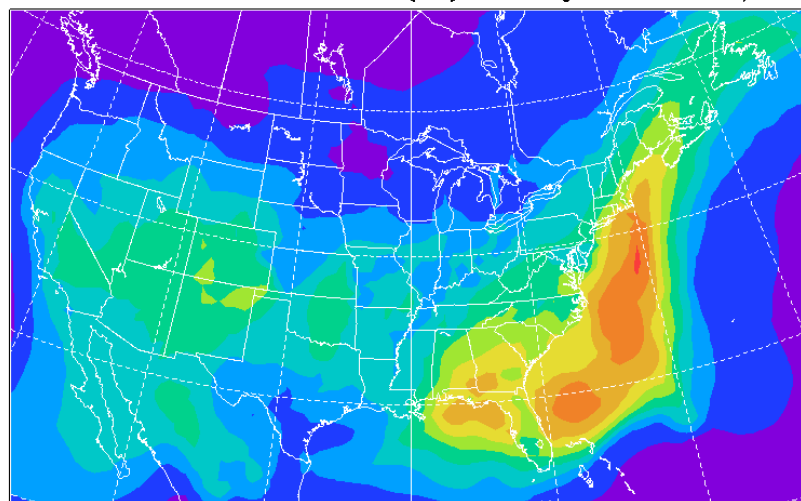


Figure 20 Average surface ozone contribution (ppbv) due to anthropogenic VOC (left) and anthropogenic CO (right), calculated as the difference between average 0-1km ozone for NEI 2001-FrostLPS-Modified, and the same in scenario in the absence of VOC and CO, respectively.

Simulated July–Average O_3 change (PANZERO–Original)/Original
in the lowest layer

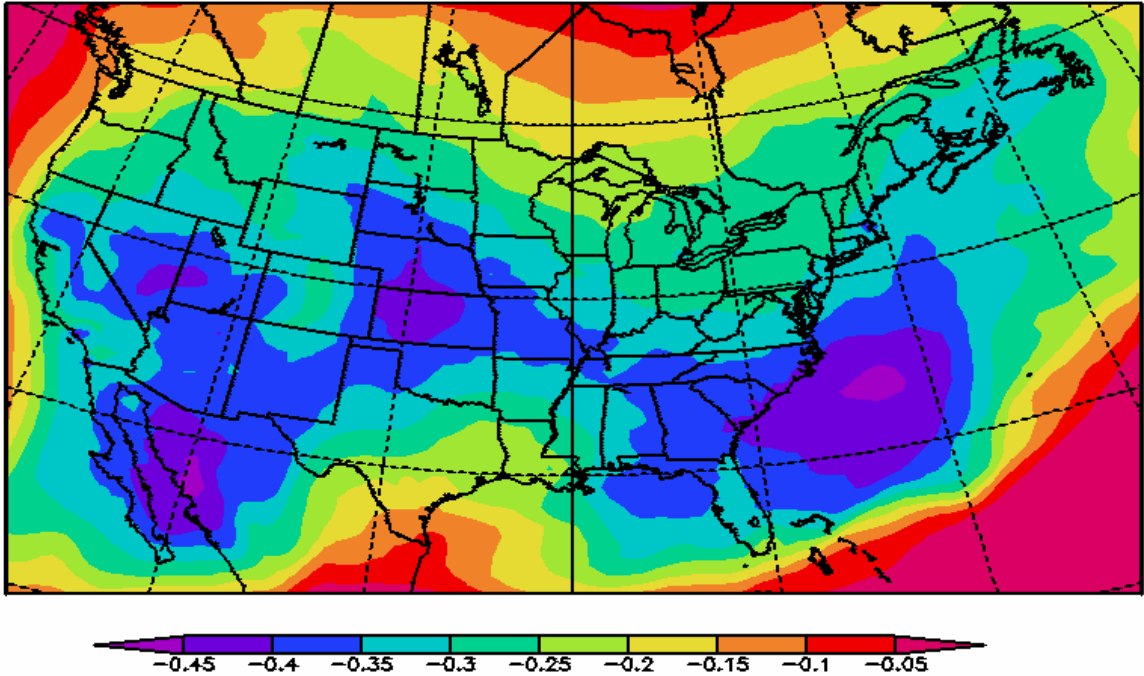


Figure 21 Calculated impact of the thermal decomposition production of NO_x on ozone. Shown are the fractional contribution to mean ozone levels at the surface for the month of July.